Master Thesis

Louise Munkholm Andreasson, Stud.cand.scient
Roskilde University, Department of Science and Environment

Autoimmune Antibody Responses towards Tau in Progressive Supranuclear Palsy

External supervisor: Tomasz Brudek, Ph.D., Cand. Scient., Senior Researcher

Internal supervisor: Karen Angeliki Krogfelt, Ph.D., Professor MSO

60 ECTS Master Thesis: August 2019 – August 2020

Submitted on 3 August 2020

ResearchLaboratory
FOR STEREOLOGY & NEUROSCIENCE

Preface and acknowledgement

This 60 ECTS master thesis was carried out at the Research Laboratory of Stereology and Neuroscience at the Bispebjerg-Frederiksberg Hospital in a time period of twelve-months, from August 1st, 2019 to August 3rd, 2020.

I would like to thank my external supervisor Tomasz Brudek for the help throughout my project with always excellent academic advice and interest. To Jonas Folke for the never-ending support whether it was a helping hand in the laboratory or a personal matter.

A huge gratitude to everybody at N-lab for providing a comfortable and friendly environment where educational experience was possible through English presentations at N-lab as well as the Lassensdag. This has opened up for meeting other academic people and visiting other departments at the Bispebjerg Hospital. Hence, I would like to thank Anne-Mette Hejl from the Department of Neurology at the Bispebjerg-Frederiksberg Hospital for the possibility to meet patients and to participate in a meeting with Hukommelses Klinikken.

To my internal supervisor Karen Angeliki Krogfelt, for supervising and showing support and great interest for my project.

Abstract

Progressive supranuclear palsy (PSP) is a progressive neurodegenerative disease characterized by intracellular aggregation of hyperphosphorylated Tau (P-Tau), tufted astrocytes, and loss of neurons resulting in movement difficulties. Naturally occurring antibodies (nAbs) have housekeeping functions and help maintain homeostasis by clearance of cell debris as well as misfolded and aggregated proteins. Impairment of this clearance system is crucial in preserving homeostasis.

We hypothesize that an immune deterioration could be an important reason for impaired clearance of pathological proteins, and a decrease in high affinity/avidity anti-Tau nAbs in PSP patients may contribute to disease progression. Low affinity/avidity nAbs may be insufficient in clearance of pathological protein, thus a decline in the binding properties of nAbs may have immunopathological implication in PSP. Therefore, our aim was to investigate the affinity/avidity of specific nAbs towards Tau in plasma from PSP patients and compare with healthy controls.

We investigated the apparent affinity/avidity of anti-Tau and anti-P-Tau nAbs in plasma samples from 55 PSP patients and 59 healthy controls using competitive Meso Scale Discovery and Enzyme-linked immunosorbent assay set-ups. We found significantly reduced levels of high affinity/avidity anti-Tau and anti-P-Tau nAbs in PSP patients compared to healthy controls. Furthermore, we found a significant increase of relative levels of anti-Tau IgG1 in plasma from PSP patients compared to healthy controls.

One interpretation is an impaired clearance system of the pathological protein, Tau, due to the lack of high affinity/avidity nAbs towards Tau. Immunotherapy with high affinity/avidity anti-Tau nAbs may be potent serve in treatment strategies for PSP patients. Furthermore, an increased relative level of anti-Tau IgG1 indicate an immune response towards Tau and may be leading to increased neuroinflammation.

Resumé

Progressiv supranucleær parese (PSP) er en progressiv neurodegenerative sygdom karakteriseret af intracellulær ophobning af hyperfosforyleret Tau (P-Tau), tab af neuroner og tuftede astrocytter som forårsager bevægelsesbesvær. Naturlig opstående antistoffer (nAbs) har housekeeping-funktioner og hjælper med at opretholde homøostase ved at fjerne celle rester, misfoldede og ophobende proteiner. Defekter i dette system ville være katastrofalt for at opretholde homøostase.

Vores hypotese om forringelse af immunesystemet kan være en vigtig rolle i oprydningen af patologiske proteiner, og derfor kunne en reducering af høj affinitet/aviditet anti-Tau nAbs i PSP-patienter være en del af sygdomsprogressionen. Hvis lav affinitet/aviditet nAbs er utilstrækkelige, i fjernelsen af patologiske proteiner, kan en ændring af nAbs' bindings egenskaber have immunopatologiske implikationer i PSP. Derfor er vores mål at undersøge affinitet/aviditet af specifikke nAbs imod Tau i plasma fra PSP-patienter og sammenligne med raske kontroller.

Vi undersøgte den tilstedeværende affinitet/aviditet hos anti-Tau og anti-P-Tau nAbs i plasma prøver fra 55 PSP-patienter og 59 raske kontroller ved at bruge en kompetitiv Meso Scale discovery og enzyme-linked immunosorbent assay opstillinger. Vi fandt en signifikant reducering af høj affinitet/aviditet anti-Tau og anti-P-Tau nAbs in PSP-patienter sammenlignet med raske kontroller. Derudover, fandt vi en signifikant øgning i den relative mængde af IgG1 anti-Tau i plasma fra PSP-patienter sammenlignet med raske kontroller.

En fortolkning af dette kan være at et dysfunktionelt oprydningssystem af det patologiske protein Tau, er mangel på høj affinitet/aviditet nAbs mod Tau. Immunterapi med høj affinitet/aviditet anti-Tau nAbs ville tjene som en potentialbehandlingsmetode for PSP-patienter. Derudover indikere en forøgelse af det relative niveau af anti-Tau IgG1 en immune respons og kan indikere en øget inflammatorisk respons i hjernen.

Contents

Abbreviation list

α-syn	α-synuclein
Aβ	Amyloid-beta
Ab	Antibody
ALS	Amyotrophic Lateral Scleroses
APC	Antigen presenting cell
BBB	Blood-brain barrier
B cells	B-lymphocytes
BCR	B cell receptor
Breg	B regulator
BSA	Bovine Serum Albumin
CNS	Central nervous system
DZ	Dark zone
ECL	Electrochemiluminescence
ELISA	Enzyme-Linked Immunosorbent Assay
GC	Germinal center
GSK-3	Glycogen synthase kinase-3
HC	Healthy control
Ig	Immunoglobin
MHC	Major Histocompatibility complex
MSA	Multiple System Atrophy
MSD	Meso-scale discovery
MT	Microtubule
MTBR	Microtubule-binding repeats
nAbs	Naturally occurring autoantibodies
NfL	Neurofilament light chain

NFT	Neurofibrillary tangles
PAMP	pathogen-associated molecular pattern
PBS	Phosphate-buffered saline
PD	Parkinson's disease
PET	Positron emission tomography
PNS	Peripheral nervous system
PP2A	Phosphatase-2A
PRD	Proline-rich domain
PRR	Pattern recognition receptors
PSP	Progressive supranuclear palsy
P-Tau	Phosphorylated Tau
RT	Room temperature
SHM	Somatic hypermutation
T cells	T-lymphocytes
TCR	T cell receptor
TDP-43	TAR DNA-binding protein 43
Th	T helper
Treg	Regulatory T cell
3R	Three microtubule-binding repeats
4R	Four microtubule-binding repeats

1. Introduction

1.1 Progressive Supranuclear Palsy

1.1.1 Epidemiology

Progressive Supranuclear Palsy (PSP) is a progressive neurodegenerative disorder, with a prevalence of 1-5 cases per 100,000 (Nath et al., 2001; "Orphanet: Progressive supranuclear palsy," 2010). The mean age of disease onset is approximately 65 years, and mean duration time is 8.5 years (Respondek et al., 2014). The diagnosis can be difficult to make and is typically confirmed (from possible to probable) three or four years after the first onset of symptoms when the cardinal features, namely falls and supranuclear gaze palsy, unambiguous appears (Höglinger et al., 2017).

1.1.2 Clinical description and treatment

PSP is an atypical Parkinsonian disorder with characteristic signs of gait and postural instability with early backward falls, supranuclear gaze palsy, cognitive impairment, and parkinsonism (Boxer et al., 2014; Dickson et al., 2007). Other symptoms of the disease are pseudobulbar signs, disturbance of eyelid movement, rigidity axial and slowed movements (Boxer et al., 2014; Levin et al., 2016). Clinical diagnosis of PSP can be problematic due to numerous PSP phenotypes (Höglinger et al., 2017), and are often misdiagnosed as Parkinson's Disease (PD) (Owolabi, 2013). The first descriptive clinical phenotype is known as Richardson's syndrome, which seems to affect ~25% of PSP patients (Armstrong, 2018; Stamelou et al., 2010). The current treatment for PSP is exclusively symptomatic to alleviate the motor symptoms (Levin et al., 2016). Therapeutic drugs targeting Glycogen synthase kinase-3 (GSK-3) and neuroprotective compounds have been tested, without significant clinical improvement (Boxer et al., 2014; Höglinger et al., 2014; Tolosa et al., 2014).

1.1.3 Neuropathology

In general PSP is considered as a sporadic disorder, and the incidence increases with age (Im et al., 2015). Pathologically, abnormal accumulation of the isoform four microtubule-binding repeats Tau (4R Tau) in neurons and astrocytes, generating neurofibrillary tangles (NFT) and tufted astrocytes in the basal ganglia, diencephalon, and brainstem. Hence, PSP belongs to the family of tauopathies (Dickson et al., 2007; Höglinger et al., 2011). Some of the functions

affected in these brain regions are responsible for motor control, oculomotor nerve, and behaviour (Basinger & Hogg, 2019; Lanciego et al., 2012). Other pathological characteristic are neuropil threads, coiled bodies in oligodendrocytes, gliosis, neuronal loss and tufted astrocytes (Figure 1) (Armstrong, 2018; Stamelou et al., 2010). Genetically, PSP is strongly associated with single nucleotide polymorphisms in the *MAPT* gene and a small number of familial PSP cases have been reported to show a overrepresentation of H1 haplotype compared to sporadic PSP (Höglinger et al., 2011; Im et al., 2015).

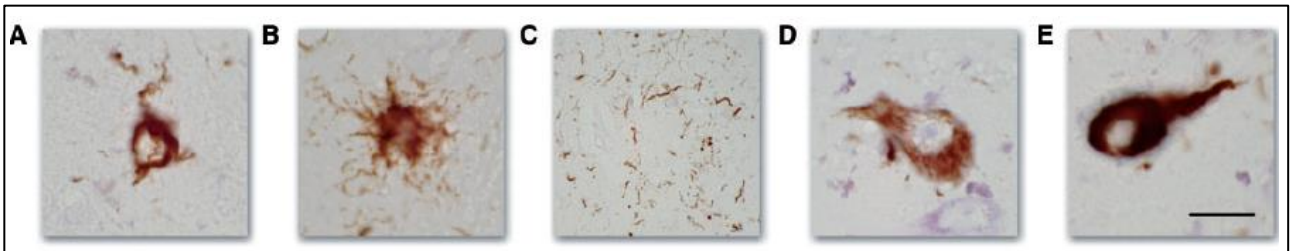

Figure 1 | ***Immunohistochemistry examination of striatum from a post-mortem PSP brain****. Human Tau protein phosphorylated specific on serine residues 396 and 404 are target by an antibody to demonstrate intracellular Tau aggregates in oligodendrocytes (**A**), astrocyte (**B**), neuropil threads (**C**), pre-neurofibrillary tangles (**D**) and neurofibrillary tangles (**E**). Modified from* Stamelou et al., 2010*.*

1.2 Microtubule-associated protein: Tau

Tau is a microtubule-associated protein contributing in neuronal functions; regulation of microtubule dynamics, participation of axonal transport and neurite outgrowth (Lacovich et al., 2017). Despite the normal function of Tau, it is a major contributor in neurodegenerative diseases, known as tauopathies (Gao et al., 2018).

1.2.1 Tau expression and structure

The human Tau is encoded by the *MAPT* gene which is located on chromosome 17p21 and consist of 16 exons, in which eight are spliced. The pre-mRNA is spliced in a manner that correlates with the type of neurons and the stage of maturation (Guo et al., 2017; Shahani & Brandt, 2002). Tau is predominantly expressed in neurons and enriched in axons in the central nervous system (CNS), although a bigger isoform is found in the peripheral nervous system (PNS) (Shahani & Brandt, 2002). In the human CNS, six isoforms of the protein are transcribed with a size range from 37-46 kDa that are generated by alternative splicing, ranging from 352 to 441 amino acids residues (Figure 2) (Guo et al., 2017; Lacovich et al., 2017). The isoforms differ in the absence or the presence of exon 2, 3, and 10; the isoforms consist of either having nil, one, or two N-terminal regions and three microtubule-binding repeats (3R) or four

microtubule-binding repeats (4R). Exon 3 is only expressed if exon 2 is presence (Figure 2). The ratio of 3R and 4R are 1:1 in the healthy adult brain, although only 3R are expressed in the developing brain (Guo et al., 2017; Wang & Mandelkow, 2016).

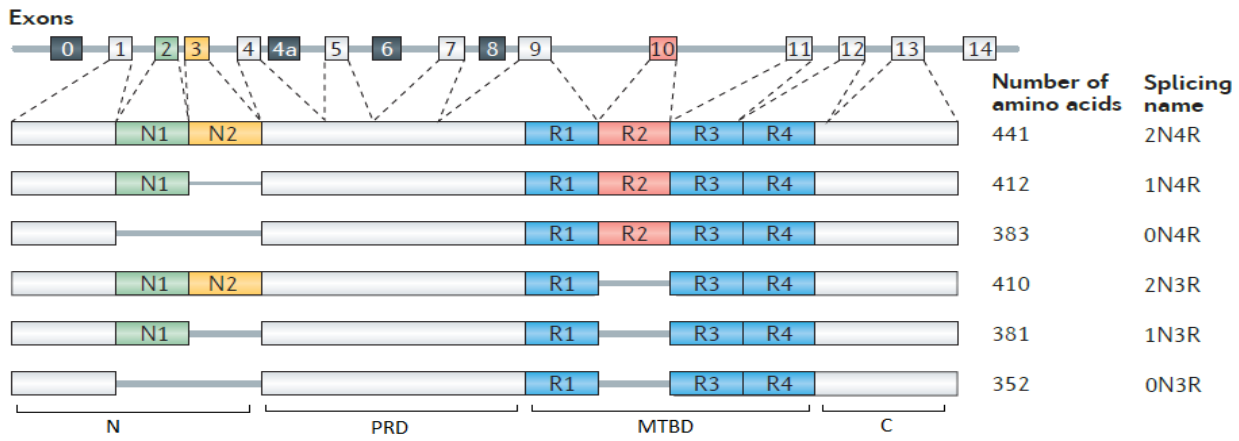

Figure 2 | ***Schematic overview of the six isoforms of Tau in the human CNS.*** *The sixteen exons are shown and which of the exons that are included in the different isoforms generated from alternative splicing. Number of amino acids are shown for each isoform as well as the splicing name, indicating the numbers of N-terminals and microtubule-binding domains included in the transcript. N = N-terminal region, PRD = proline-rich domain, MTBD = microtubule-binding domain, C = C-terminal. Modified from* Shahani & Brandt, 2002.

Tau can be subdivided into four major domains due to their biological properties (Figure 2); the N-terminal, the proline-rich domain, microtubule-binding domain, and the C-terminal. Tau have an overall hydrophilic property with a low hydrophobic portion. With a highly flexible conformation and lack a well-defined secondary and tertiary structure, Tau is classified as natively unfolded protein (Guo et al., 2017).

The microtubule-binding domain consist of motif repeats separated by flanking regions; the second and third repeats have a tendency to form ordered β-sheet structures. It is proposed that the folding of free Tau have a conformation as a "paperclip", where the C-terminal folds over the microtubule-binding domain and the N-terminal folds over the C-terminal, whereas during interaction with microtubules the "paperclip" conformation opens (Figure 3) (Guo et al., 2017).

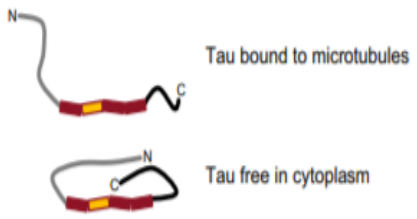

Figure 3 | ***Schematic overview of Tau in a bound and unbound conformation.*** *The microtubule-binding domain (red and yellow) binds to the microtubule and the projecting N-terminal domain (grey) creates the flanking region. The conformation of Tau differs when bound to the microtubule or as a free protein. The unbound Tau have a "paperclip" like conformation with the termini in close proximity, where the Tau conformation, when bound, opens the "paperclip". Modified from Guo et al., 2017.*

1.2.2 A part of the cytoskeleton framework: The function and regulation of Tau

The axonal and somatodendritic compartment are one of the characteristic features of neurons, and to generate the structural and functional compartmentalization, a complex intracellular structure is needed. The cytoskeleton is a major determinate in the morphology of neurons and it provides the structural framework for the axonal and somatodendritic compartments (Shahani & Brandt, 2002). The shape and structure of the cytoskeleton is enabled due to mechanical properties from actin, intermedia filament and microtubule (MT) (Desai & Michison, 1997). MTs are highly dynamic polymers and are important for growth, migration, and polarity in neurons (Pellegrini et al., 2017). Tau is a MT stabilization protein, protecting MTs against depolymerization by decreasing tubulin dissociation in both ends of MT, promoting increased growth rate and decreasing the catastrophic frequency as well as promoting bundle forming of MT (Figure 4). These bundles are involved in trafficking vesicles and organelles between the cell compartments in collaboration with other proteins (Barbier et al., 2019; Venkatramani & Panda, 2019).

Posttranslational modification of Tau is a regulator mechanism which specifies the function and location, affecting the physiological properties of Tau. There are numerous posttranslational modifications including phosphorylation, acetylation, glycation, and nitration (Heinisch & Brandt, 2016; Trushina et al., 2019). Phosphorylation has been the most studied modification due to association with many neurodegenerative disorders; hence this modification will be discussed below. Phosphorylation of Tau decreases the binding to MT, thereby reducing the stability of MT (Guo et al., 2017). During embryogenesis and early development only 3R Tau is expressed in the fetal brain. 3R Tau in the foetal brain has a lower affinity to MT and is highly phosphorylated, compared to the adult brain which present all six isoforms in a less phosphorylated state. The increased phosphorylation of Tau in the fetal brain might be a result for greater neuronal plasticity (Hanger et al., 2009). Tau phosphorylation is dynamically regulated by different kinases and phosphatases, including GSK-3 and phosphatase-2A (PP2A) (Noble et

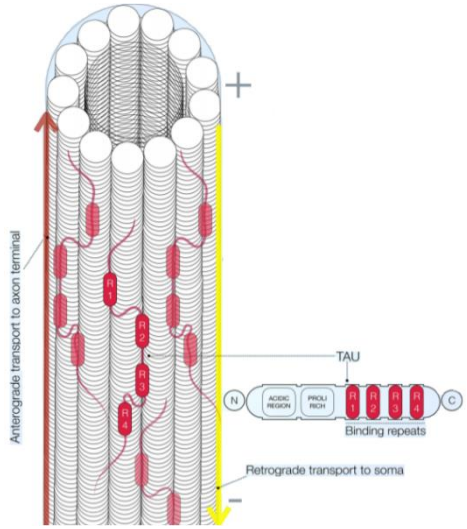

*Figure 4 | **Schematic overview of microtubule bundle formation with Tau.** Tau (red) is interacting with microtubules to promote microtubule bundles (white). Red arrow indicates the anterograde transport. Yellow arrow indicates the retrograde transport. Modified from Pellegrini et al., 2017.*

al., 2013), to maintain a normal level of phosphorylated Tau as well as proper structure and function (Gong & Iqbal, 2008). Tau contains 85 possible phosphorylation sites which comprises of 45 serines, 35 threonines, and 5 tyrosines (Hanger et al., 2009) representing 20% of the protein. Numerous of these residues are mainly located in the proline-rich domain (PRD), and the C-terminal; phosphorylation at these residues can affect the activity in stabilising MT assembly by increasing or decreasing binding to tubulin, or self-aggregation. Phosphorylation of the C-terminal promotes a higher self-aggregation than phosphorylation at the PRD (Liu et al., 2007).

1.2.3 Tau pathology – clinical significance

The pathological hallmark of PSP is aggregation and accumulation of hyperphosphorylated Tau, and the underlying mechanism which trigger this dysregulation of Tau is still unknown (Shoeibi et al., 2019). Many possible phosphorylation residues are located on the protein, where ten of these residues have been found to be phosphorylated on soluble Tau and least 16 residues have been found to be phosphorylated on insoluble Tau in PSP patients and 45 residues in Alzheimer's disease (Hanger et al., 2007; Noble et al., 2013; Wray et al., 2008). An imbalance in the numerous kinases and phosphatases that regulates phosphorylation of Tau is believed to result in highly phosphorylated Tau (Noble et al., 2013). Rydbirk et al., 2019 showed an upregulation of GSK-3β mRNA in prefrontal cortex in PSP patients compared to controls and another research group showed a upstream regulation of PP2A contributed in dysregulation of the phosphatase (Park et al., 2018). These findings suggest dysfunction of the regulatory mechanisms of Tau can contribute to Tau pathology in PSP and other neurodegenerative disorders. Hyperphosphorylated Tau are responsible for loss of function by self-aggregating forming NFT and hinder the interaction with MT. Loss of function promote gain of toxicity by preventing binding of other MT-associated proteins and spread of Tau from a donor cell to a recipient cell which generates new "seeds" of Tau. It is suggested that this seeding process promote formation of Tau oligomers which are thought to be the toxic species in the brain (Liu et al., 2007; Spires-Jones et al., 2017). Site-specific phosphorylation can alter assembling of MT and promote self-aggregation in different levels, and Liu et al., 2007 showed GSK-3β phosphorylates residues in the C-terminal which promoted an increase in MT assembling but had a higher self-aggregation, compared to kinases phosphorylating the PRD. Neuroinflammatory processes are suggested to be part of the disease course, nonetheless a

knowledge gap exists in how neurodegenerative disorders, like PSP, are affected by neuroimmunomodulating factors (Rydbirk et al., 2019).

1.3 Immune system

The immune system is the body's defence system against pathogens. This system is highly evolved to recognize self from non-self and is able to obtain a suitable environment for the commensal organisms in the body. The immune system is divided in two: the innate immune system and the adaptive immune system that are the first and second line of defence, respectively (Chaplin, 2010; Hato & Dagher, 2015).

1.3.1 Innate immune system

The innate immune system is the first response towards an invading pathogen. It is a conserved system that consist of several different cellular components (Figure 5); phagocytic cells, antigen presenting cells, killing cells, cytokines, chemokines, and the complement system. The system has evolved a specialised recognition pattern which enabled recognition of nonself from self. Immune cells have specific membrane-bound receptors, i.e. Toll-like receptors, known as pattern recognition receptors (PRR), which recognise specific structures on pathogens, so called pathogen-associated molecular patterns (PAMPs). PRR are encoded in the germline which limits the variety of pathogen recognition (Hato & Dagher, 2015; Kawai & Akira, 2011). When PAMPs are recognized by PRR, the exogenous pathogen is engulfed and processed in the immune cell which can then travel to the secondary lymphoid organs to present the antigen. An important connection between the innate and adaptive immune system are the antigen presenting cells (APCs); dendritic cells (DC) and macrophages which can present antigens through a specialized receptor, major histocompatibility complex (MHC) (Saiz et al., 2018).

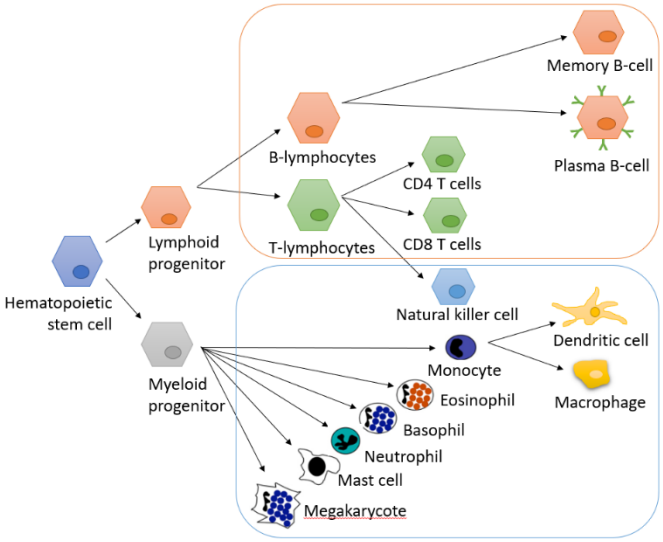

*Figure 5 | **Schematic overview of the immune cells**. Immune cells from the innate immune system (blue box, lower right) and adaptive immune system (red box, upper right). Hematopoietic stem cells differentiate into myeloid or lymphoid progenitor which further differentiate. Modified from Chaplin, 2010.*

1.3.2 Adaptive immune system

The adaptive immune system has evolved a more efficient way to recognise pathogens and generates a specific immune response. Contrary to the innate system, the cellular components of the adaptive system memorize the encounter with a specific antigen, also known as epitope, which can generate a faster and greater response towards a pathogenic antigen if a re-encounter occurs. The specific immune response is enabled due to the production of specific immune cells which have different specificities for pathogenic antigens. The memory in the adaptive immune response rises from antigen-specific lymphocytes: B-lymphocytes (B cells) and T-lymphocytes (T cells) (Figure 5). These cells have an encoded gene segment for antigen-specific receptor that through irreversible gene rearrangement and DNA recombination can produce receptors compatible with an antigen. When the antigen-specific receptor encounters a compatible antigen it will activate the cell, to produce progeny with the same gene rearrangement, activate other immune cells, or elimination of the pathogen (Murphy & Weaver, 2016; Natoli & Ostuni, 2019; Wood, 2011).

1.3.2.1 T-lymphocytes

One of the major players in adaptive immunity are the T cells, which can be divided into $CD4^+$ and $CD8^+$ T cells. T cells are produced in the bone marrow from a common precursor cell that originates from hematopoietic stem cell (Figure 5), but maturation of the T cells happens in the thymus. Through maturation the cells become either $CD4^+$ or $CD8^+$ T cells, which are expressed through a heterodimeric T cell receptor (TCR) that comprises of α and β chains. Naive T cells travel to the secondary lymphoid organs, where they can be activated by APCs. (Vacchio & Bosselut, 2016). APCs with MHC class I/antigen complex will activate $CD8^+$ T cells with the compatible TCRs, to become effector T cells and proliferate. These effector T cells migrate to infected peripheral sites due to secreted chemokines, to eliminate infected cells and release cytokines (Vacchio & Bosselut, 2016; Zhang & Bevan, 2011). APCs activates $CD4^+$ through MCH class II/antigen complex with the compatible TCRs, to become a T helper (Th) cell and proliferate. Th cells interact with both $CD8^+$ T cells and B cells, and Th cells are essential in B cell germinal center formation (Figure 6), antibody maturation, and class switching (MacLeod et al., 2010; Petersone et al., 2018). Another cell type derived from the $CD4^+$ linage is the regulatory T cells (Tregs) that function as potent immunosuppressive cells. Treg cells are able to constrain T cell proliferation, cytokine production, and control immune homeostasis (Kondělková et al., 2010; Workman et al., 2009).

1.3.2.2 B-lymphocytes

The second major player in adaptive immunity are B cells, which are developed from a common precursor cells that originate from hematopoietic stem cells (Figure 5). Contrary to T cells, the maturation of B cells happens in the bone marrow in which they become naive B cells. The early stages for B cell maturation is characterized through expression of cell surfaces markers and immunoglobin (Ig) with a successive rearrangement of the heavy and light chains. Immature B cells express IgM and IgD on their surface and these B cell receptors (BCR) are examined for autoreactivity before migrating to secondary lymphoid organs for final maturation (Eibel et al., 2014; Shi et al., 2019). In the secondary lymphoid organs, through a specialized microstructure known as the germinal center (GC) the final B cell maturation can happen. Within the GC, high affinity antibody (Ab) secreting B cells and memory B cells are developed. Through somatic hypermutation (SHM) of genes encoding the BCR, a large variety of BCRs can be produced. To ensure a selection for BCRs with high affinity for an antigen without any cross reactivity to self, the GC is tightly regulated by DCs and Th cells. The GCs are divided in the dark zone (DZ), where B cells proliferate and undergoes class switch recombination due to SHM, and in the light zone where B cells capture an antigen through follicular DCs and present with MHC class II/antigen complex to Th cells for positive selection. After positive selection B cells re-enter the DZ for proliferation and SHM before becoming a long-lived antibody secreting cells or memory B cells (Figure 6) (Eibel et al., 2014; Stebegg et al., 2018). This process is well known as a T cell-dependent immune response, although B cells can differentiate into plasma cells with low affinity Ig upon a strong antigen stimulation, which is known as T cell-independent immune response (Seifert & Küppers, 2016). These maturation processes creates a population of

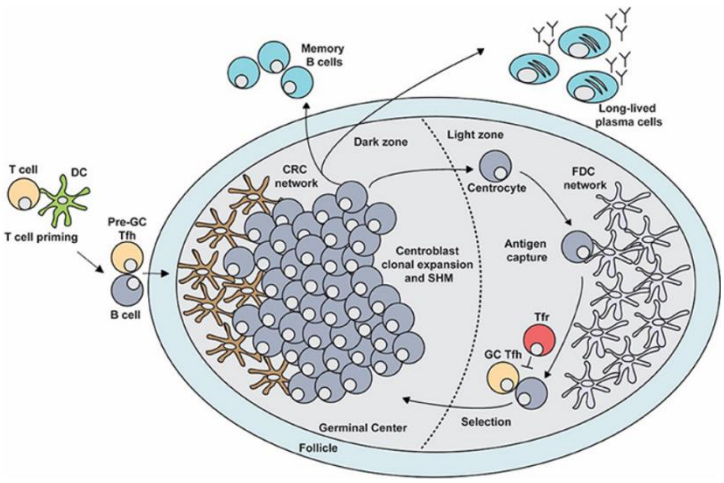

*Figure 6 | **The germinal center (GC) response.** B cells follicles of secondary lymphoid organs are specialized microstructure, known as GC, within B cells can undergo final maturation. The GC comprises of two compartments, the dark zone (DZ) and the light zone (LZ). In the DZ B cells undergo proliferation and somatic hypermutation (SHM). In the LZ, follicular dendritic cells (FDC) present antigen which is captured by the B cells and is then incorporated, processed and presented to follicular T helper (Tfh) cells in order to undergo positive selection. Then B cells re-enter the DZ for another round of proliferation and SHM before exiting the GC as long-lived plasma B cell or memory B cell. B cells are referred to as centroblast in the DZ and centrocyte in the LZ in the figure. Figure from Stegbegg et al., 2018.*

conventional B-2 cells (Rothstein et al., 2013). During ontogenesis a subset of B cells are generated; B-1 cells that are long-lived, self-renewing, and are found in the primary and secondary lymph organs as well as in the blood, peritoneal and pleural cavities. B-1 cells have a receptor repertoire towards bacteria and self-antigens promoting a rapid response towards infectious bacteria and clearance of cell debris. B1-cells produces natural polyreactive antibodies with a broad autoreactive repertoire (Holodick et al., 2017; Palma et al., 2018; Wong et al., 2019). Another subset of B cell is the regulatory B (Breg) cells in which pro-inflammatory cytokines have a crucial role in the differentiation but are still poorly understood. Bregs exhibit immunosuppressive functions by releasing cytokines and contribute in the immunological tolerance (Menon et al., 2016).

1.3.2.2.1 Immunoglobins

Igs are also referred to as antibodies (Abs) which are Y-shaped protein consisting of more functional components which include two antibody-binding domains (Fab) linked to a hinge region which can give a large degree of flexibility relative to the fragment interacting with the cell surface (Fc) (Figure 7). Fabs are composed of the light and heavy chain variable regions as well as one constant region, whereas Fc region is composed of only the heavy chain constant regions. The heavy and light chains are linked by disulfide bridges. The heavy chain can contain more than one constant region depending on the Ig isotype. Five isotypes of Igs exist depending of the number of heavy chain constant regions; IgA, IgD, IgE, IgG, and IgM in which each have independent roles in the adaptive immunity. IgA and IgM contain additional chains allowing formation of dimers and pentamers, respectively (Chiu et al., 2019). Igs are proficient of recognizing a broad variety of antigens which is due to the specificity and diversity of the antigen-binding sites that are developed during the B cells maturation (Shi et al., 2019). The antigen will bind the Ig at the antigen-binding site that are formed in Fab, and

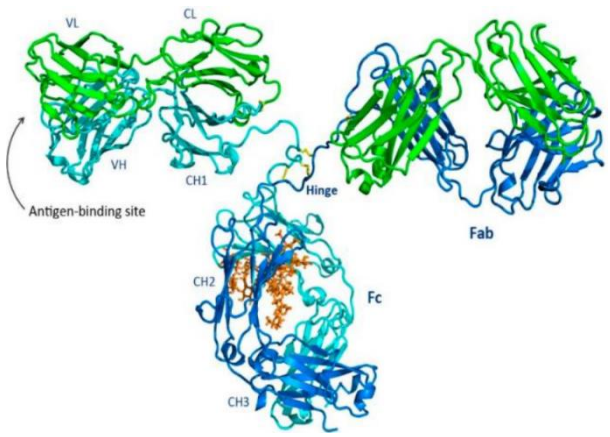

*Figure 7 | **Ribbon representation of immunoglobin (Ig).** The antigen-binding site is located at the N-terminal within the variable regions of the heavy (cyan) and light (green) chain. The constant region for the light chain (CL) and the constant region of the heavy chain (CH1) together with the variable regions are part of the fragment antigen-binding domain (Fab). The hinge region (yellow) allow the Fabs to have a large degree of flexibility relative to the fragment crystallized (Fc) consisting of the heavy chain constant regions 2 and 3 (CH2 or CH3). Figure from Chiu et al., 2019.*

the Fc is the functional part which determines how to process the antigen if it is compatible with the antigen-binding site (Chiu et al., 2019). Ig can also act as an opsonin, generating a more favorable phagocytosis (Winkelstein, 1973).

1.3.3 Naturally occurring antibodies – clearance system

Naturally occurring antibodies (nAbs) are secreted by B-1 cells and are formed in germ-free conditions and absence of exogenous antigens. Hence, resulting in less hypermutations and affinity maturation, giving nAbs lower affinity than conventional B-2 cell Abs. Although B cells are part of the adaptive immunity, nAbs contribute to the first line of defence towards exogenous pathogens (Holodick et al., 2017; Kronimus et al., 2018; Palma et al., 2018). nAbs are polyreactive, recognize self-antigen, and have a low affinity towards exogenous pathogens. nAbs present a great portion of Abs in the human body and are part of a clearance system which involves maintaining of homeostasis through removal of cell debris, damaged, aggregated or misfolded proteins (Gold et al., 2012; Kronimus et al., 2018; Palma et al., 2018). Autoreactive IgMs have a pivotal role in clearing apoptotic cells and in preventing autoimmunity. IgM binds to the cell and works as an opsonization for immature DC or macrophages to recognize and engulf the cell. Recruitment of C1 protein from the classical complement pathway can enhance the phagocytosis of apoptotic cells. The phagocytosis by immature DC enables self-antigens presentation and induces immunological tolerance (Chen et al., 2009; Holodick et al., 2017). IgG can further be divided into four subclasses; IgG1, IgG2, IgG3, and IgG4 which are named according to decrease in abundance. In addition, IgG1-4 subclasses generate Ab responses towards different types of antigens that differ in complement activation, triggering of effector cells, and immune complex formation (table 1) (Vidarsson et al., 2014). nAbs have been shown to inhibit and reduce aggregation of disease-associated proteins in neurodegenerative diseases (Albus et al., 2018), which make nAbs a potential approach for a therapeutic strategy. In neurodegenerative diseases an altered level of nAbs towards disease-associated proteins have been shown (Folke et al., 2019; Kronimus et al., 2016), which could have potential as a biomarker for diagnostics.

Table 1 | *Properties of IgG subclasses and IgM in humans.*

	IgG1*	**IgG2***	**IgG3***	**IgG4***	**IgM#**
General					
Molecular mass (kDa)	146	146	170	146	900
Mean adult serum level (mg/dl)	698	380	51	56	50-250
Relative abundance (%)	60	32	4	4	
Antibody response to					
Proteins	++	+/-	++	++	
Polysaccharides	+	+++	+/-	+/-	++
Allergens	+	(-)	(-)	++	
Complement activation					
C1 binding	++	+	+++	-	+++

* Adapted from (Vidarsson et al., 2014).

Adapted from (Sathe & Cusick, 2020)

2. Hypothesis

From previous studies performed at the Laboratory for Stereology and Neuroscience, the clearance of pathological proteins such as α-synuclein (α-syn) and TAR DNA-binding protein 43 (TDP-43), was shown to be impaired due to an insufficient/absent concentrations of antigen specific nAbs in PD patients, Multiple System Atrophy (MSA) patients (Brudek et al., 2017), and Amyotrophic Lateral Sclerosis (ALS) patients (Kallehauge et al., in review) compared to healthy controls.

We hypothesize that an impaired humoral immunity (possible B cell defects) resulting in Ab affinity/avidity deficiencies can lead to impaired clearance Tau aggregates, and elimination of damaged brain cells leading to neuroinflammation and neurodegeneration in PSP patients.

2.1 Main aims

1. To investigate affinity/avidity of anti-Tau and anti-P-Tau nAbs towards Tau or P-Tau in plasma samples from PSP patient and healthy controls using competition assay on MSD platform.
2. To measure relative levels of IgG1-4 subclasses, total IgG, and IgM towards Tau in plasma samples from PSP patients and healthy controls using indirect ELISA.
3. To estimate global levels of IgG1-4 subclasses, total IgG and IgM in plasma samples from PSP patients and healthy controls using commercially available ELISA kits.

3. Material and Methods

3.1 Material for Meso-Scale Discovery (MSD) platform

Equipment

MSD Sector Imager S600 instrument (MSD)

96-well plate High-bind MSD plate, Cat. No. L15XB-3 (MSD)

96-well plate Standard MSD plate, Cat. No. L15XA-3 (MSD)

Reagents

Phosphate Buffer (PBS), pH 7.4 (Apoteket RegionH, Denmark)

Carbonate-Bicarbonate Buffer, Cat. No. C3041-50CAP (Sigma Aldrich)

Bovine Serum Albumin (BSA) Fraction V, Cat. No. 05482-100G (Sigma Aldrich)

Tween-20, Cat. No. 9005-64-5 (Sigma Aldrich)

MSD Read Buffer T (4X) With Surfactant, Cat. No. R92TC-2 (MSD)

SuperBlock™ Blocking Buffer in PBS, Cat. No. 37515 (TermoFisher)

Buffer solutions

Coating buffer: Carbonate capsule + 100 mL distilled water, pH 9.5.

Dilution buffer: PBS + 0.1% BSA Fraction V

Washing buffer: PBS + 0.05 % Tween-20

Reading buffer: MSD Read Buffer + distilled water (1:2)

Antigens

Tau-441 (2N4R) (100 µg/ml), molecular weight 49.5 kDa. Human Tau isoform 441 sequence, recombinant protein expressed in *E. coli*, Cat. No. T-1001-2 (rPeptide).

Tau-441 TTBK1-phosphorylated (P-Tau) (100 µg/ml), molecular weight 64kDa. Human recombinant Tau-411 co-expressed with TTBK1 in *E. coli*, Cat. No. T08-50ON (SignalChem).

TDP-43 (1 mg/ml), molecular weight 48.8 kDa. Human recombinant TARDBP protein expressed in *E. coli* and fused to His-tag at N-terminus, Cat. No. ATGP2093 (NKMAX).

α-synuclein (1 mg/ml), molecular weight 14.5 kDa. Human recombinant α-synuclein protein expressed in *E. coli*, Cat. No. S-1001-2 (rPeptide).

Secondary antibody

MSD SULFO-TAG™, Goat Anti-Human IgG Antibody, Cat. No. R32AJ-1 (MSD)

3.2 Material for indirect ELISA

Equipment

ELISE plater reader, MULTISKAN FC (Termo Scientific)

ELISE plate washer, WELLWASH (Termo Scientific)

96-well plate, MAXISORP NUNC-IMMUNO PLATE, Cat. No. 439454 (Termo Scientific)

Reagents

Phosphate Buffer (PBS), pH 7.4 (Apoteket RegionH, Denmark)

Carbonate-Bicarbonate Buffer, Cat. No. C3041-50CAP (Sigma Aldrich)

Bovin Serum Albumin (BSA) Fraction V, Cat. No. 05482-100G (Sigma Aldrich)

Tween-20, Cat. No. 9005-64-5 (Sigma Aldrich)

Tergitol® solution, Type NP-40, Cat. No. NP40S (Sigma Aldrich)

TMB ONE® ELISA HRP Substrate, Cat. No. 4380 A (ECO-TEK®)

Titripur® Sulfuric acid, Cat. No. HC85637873 (Merck)

Streptavidin-Peroxidase, stock 1 mg/ml Cat. No. S5512 (Sigma)

Buffer solution

Coating buffer: Carbonate capsule + 100 mL distilled water, pH 9.5.

Dilution buffer: PBS + 0.1% BSA Fraction V

Blocking buffer: PBS + 3% BSA Fraction V

Washing buffer: PBS + 0.1 % Tween-20

Antigen

Tau-441 (2N4R) (1 mg/ml), molecular weight 49.5 kDa. Human Tau isoform 441 sequence, recombinant protein expressed in *E. coli*, Cat. No. T-1001-2 (rPeptide).

Tau-441 TTBK1-phosphorylated (P-Tau) (100 µg/ml), molecular weight 64kDa. Human recombinant Tau-411 co-expressed with TTBK1 in *E. coli*, Cat. No. T08-50ON (SignalChem).

Secondary antibody

Monoclonal anti-Human IgG1 biotin conjugated, produced in mouse, Cat. No. MH1515 (Invitrogen)

Monoclonal anti-human IgG2 biotin conjugated, produced in mouse, Cat. No. B3398 (Sigma)

Monoclonal anti-human IgG3 biotin conjugated, produced in mouse Cat. No. B3523 (Sigma)

Monoclonal anti-human IgG4 biotin conjugated, produced in mouse Cat. No. B3648 (Sigma)

IgG total (500 µg, 0.5 mg/ml), goat pAb to Hu IgG (HRP conjugated), Cat. No. ab98717 (Abcam)

Anti-human IgM (μ-chain specific) biotin antibody produced in goat, Cat. No. B1265 (Sigma)

Secondary antibody for standard curve

HRP anti-Tau, 419-433 Antibody, (0.5 mg/ml), host species rat, monoclonal, Cat. No. 851003 (Nordic Biosite)

Polyclonal Rabbit Anti-Human Tau, stock 6.2 g/L, Cat. No. A0024 (DAKO)

Biotinylated Anti-Rabbit IgG (H + L) affinity purified, host species goat, stock 1.5 mg/ml, Cat. No BA-1000 (Vector Laboratories)

3.3 Study cohort: PSP patients and Healthy subjects

In this study, plasma samples were obtained from 55 PSP patients and 59 healthy subjects. Normal healthy subjects are referred to as healthy controls (HC) in the method and results sections. All samples were received from Movement Disorders Biobank at Bispebjerg-Frederiksberg Hospital, Copenhagen, DK. All PSP diagnoses were assigned by an experienced movement disorder specialist from the tertiary Movement Disorders Centre at the Department of Neurology, Bispebjerg-Frederiksberg Hospital, blinded to laboratory results, and all included patients met the clinical criteria (Höglinger et al., 2017) for possible or probable diagnosis at the sampling. Approval for this research study was permitted by the Ethics Committee for Copenhagen Regional Area (H-16025210) and all participants gave written informed consent for participation. Demographic characteristics are summarized in table 2.

Table 2 | *Demographic and clinical characteristics of healthy controls and progressive supranuclear palsy.*

	PSP patients (N = 55)	Healthy controls (N = 59)	P-values
Age [years] (mean)	54-81 (68.6)	58-90 (69.9)	
[SD]	[5.7]	[8.1]	0.29 *
Gender			
Female/Male	18/37	27/32	0.11 #
Age at onset [years] (mean)	47-76 (63.2)		
[SD]	[7]	-	-
Disease duration [years] (mean)	1-14 (5.3)		
[SD]	[3.3]	-	-
Hoehn and Yahr scale [years] (mean)	2-5 (3.4) ¤	-	-
[SD]	[0.69]		

All clinical data for PSP patients is presented in appendix 1
* **Unpaired t-test**
# **Chi-squared test**
¤ **Fifteen patients did not have a Hoehn and Yahr score**

3.4 Treatment of blood samples

Venous blood was drawn and processed the same day at the respective clinic, the Bispebjerg Movement Disorders Biobank, the Bispebjerg-Frederiksberg Hospital. Blood samples were collected in EDTA coated polypropylene tubes and spun down at 2000 x *g* for 10 min at 4 °C; to

remove cells and cell debris. The supernatant plasma was aliquoted and stored in 400 µl polypropylene tubes at –80°C until the day of analysis and thawed on ice.

3.5 The principles of Meso-Scale discovery (MSD) platform

MSD is similar to the traditional Enzyme-Linked Immunosorbent Assay (ELISA). However, MSD assay is more sensitive, provide larger dynamic range and uses minimal sample. The principle of MSD is light that is emitted due to electrochemiluminescent labels (Figure 8). MSD plates are coated with an antigen, e.g. Tau monomer, which is then captivated on the surface overnight. The plate is treated stepwise with blocking buffer, the given samples, and a electrochemiluminescent labeled secondary antibody (MSD, 2014). At the final step before reading the plate, MSD Read Buffer is added to the wells, which is an optimized buffer that provides a superior sensitivity, low background and high signal due to light generating co-reactant (MSD, 2019). The MSD plates are provided with electrodes in the wells, and the imager applies voltages to the electrodes, causing the SULFO-TAG close to the bottom to emit light through a series of reduction and oxidation reactions (Figure 8). The intensity of the emitted light is measured and provides quantitative measures of the samples for analysis (MSD, 2014).

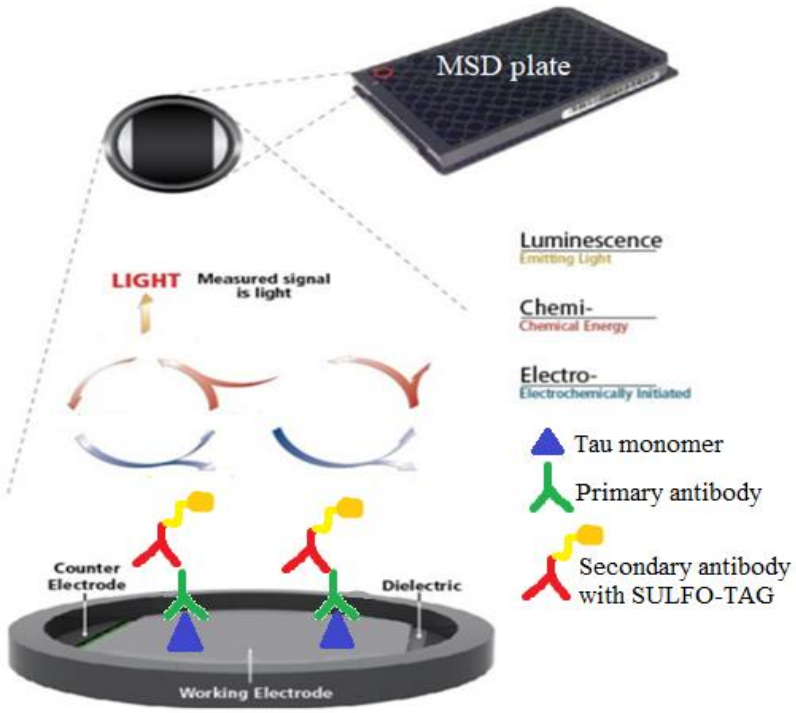

*Figure 8 | **Schematic overview of the Meso-Scale Discovery plate.** Showing the electrodes on the bottom of the well and the reactions emitting light for quantitative measurement. The captivated Tau monomers are interacting with the primary antibody against Tau and when treated with secondary antibody it will bind to the primary antibody. Appling MSD read buffer and voltage to the plate, reduction and oxidation reaction will occur and emit light. Modified from MSD, 2014.*

3.6 MSD competition assay

Affinity/avidity of anti-Tau nAbs in plasma samples from PSP patients and HCs were measured using the competition assay (Figure 9), previously developed at the Laboratory for Stereology and Neuroscience, the Bispebjerg-Frederiksberg Hospital in 2017 and adapted for this study (Brudek et al., 2017). The plasma samples comprise a mixture of polyclonal antibodies; these Abs differ in epitope specificities and affinities. When incubating the plasma samples with an increasing concentration of free Tau monomers, creating a competition reaction, it is possible to measure the Ab titer on the plate with immobilized Tau. In the fluid phase, during the incubation time, high affinity Abs bind and make more stable complexes with the antigen than low affinity Abs. Hence, low concentration of free Tau monomer efficiently inhibits high affinity Abs, and low affinity Abs are efficiently inhibited in high concentration of free Tau monomer. The low affinity Abs, that are bound to the antigen on the plate, are then tagged with secondary Abs conjugated with a SULFO-TAG and are then quantified by the MSD Sector Imager S600 instrument (Brudek et al., 2017).

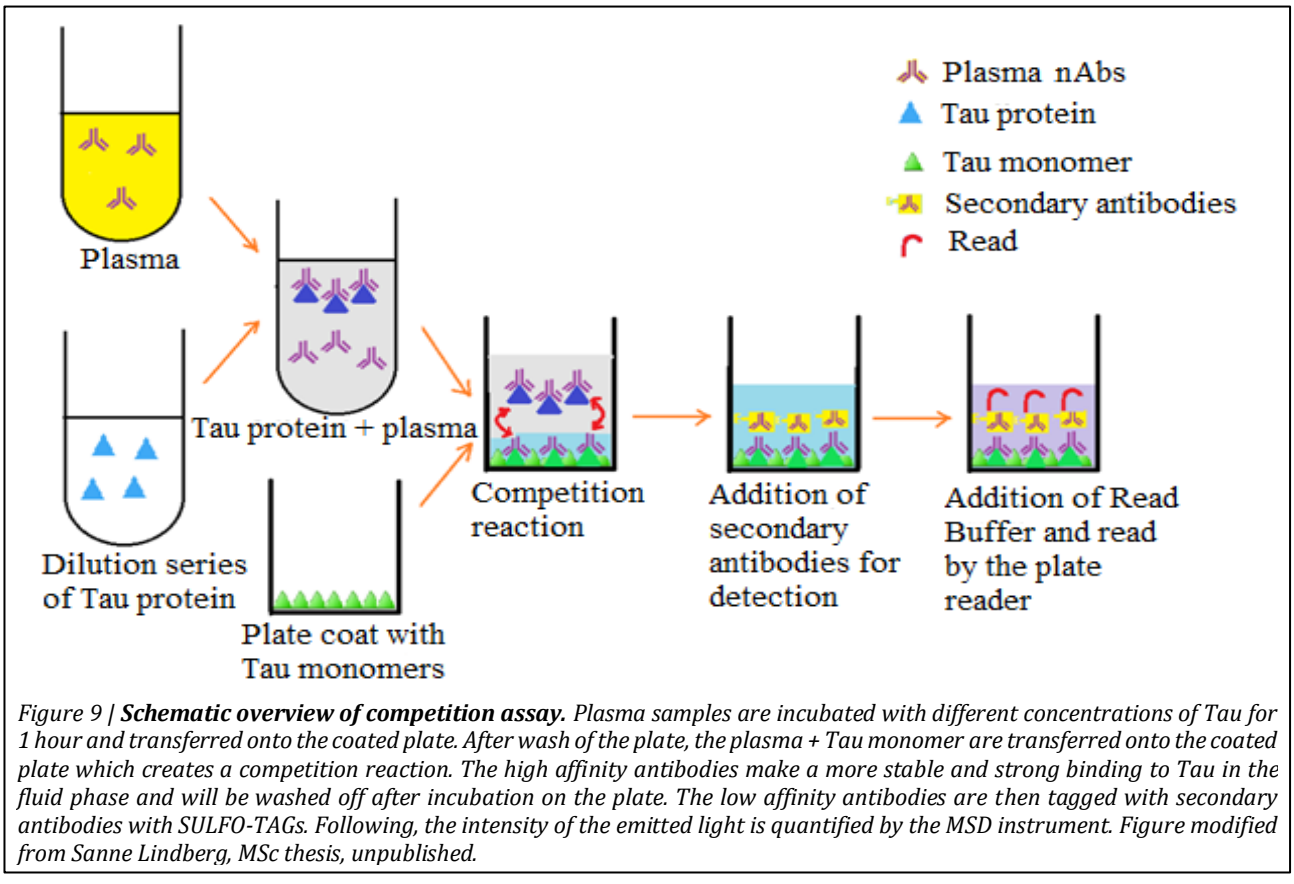

Figure 9 | ***Schematic overview of competition assay.*** *Plasma samples are incubated with different concentrations of Tau for 1 hour and transferred onto the coated plate. After wash of the plate, the plasma + Tau monomer are transferred onto the coated plate which creates a competition reaction. The high affinity antibodies make a more stable and strong binding to Tau in the fluid phase and will be washed off after incubation on the plate. The low affinity antibodies are then tagged with secondary antibodies with SULFO-TAGs. Following, the intensity of the emitted light is quantified by the MSD instrument. Figure modified from Sanne Lindberg, MSc thesis, unpublished.*

3.7 Optimization of MSD competition assay with pooled plasma samples

In preliminary experiments 10 randomly selected plasma samples from PSP patients and HCs were blended into two pools. Before proceeding to the individual samples, pools were used to determine an appropriate plasma dilution for the inhibition assays, as well as evaluating the concentration of Tau for coating the plates and plasma inhibition, see table 3.

Table 3 | *The range of Tau coating concentrations in ng/ml per well, and the different plasma dilutions diluted in PBS + 0.1 % BSA.*

Range of Tau coating concentration in ng/ml										
0.01	0.1	0.5	1	10	50	100	500	1000	5000	10,000
Plasma dilutions										
1:100		1:200		1:500		1:1000		1:2000		

Two blocking buffers were tested for optimal plate blocking result: 3 % BSA Fraction V diluted in PBS and SuperBlock™ Blocking Buffer. These conditions were evaluated on two different MSD plates: standard and high bind MSD plates. For the inhibition curve a range of dilution series of Tau, with the highest concentration of 100 nM with a 3-fold dilution or 250 nM with a 2-fold or 3-fold dilution were prepared, see table 4.

Table 4 | *Different dilution series of Tau monomers for inhibition assays in a 2- or 3-fold dilution, with a starting concentration of 100 nM or 250 nM, all concentrations of Tau are given in nM.*

3-fold dilution	**2-fold dilution**	**3-fold dilution**
100	250	250
33	125	83.3
11	62.5	27.8
3.7	31.3	9.3
1.2	15.6	3.1
0.4	7.8	1.03
0.1	3.9	0.34
0.0	0.0	0.0

For assay optimization with P-Tau on high bind plates, SuperBlock™ Blocking Buffer and similar plasma dilution were used to be as comparable to the settings for Tau. Different coating concentrations of P-Tau and concentrations for the dilution series of P-Tau monomers for the inhibition assay were examined, table 5. All concentrations are examined based on results obtain from examination of Tau.

Table 5 | *The different P-Tau coating concentrations in ng/ml. Different dilution series of P-Tau monomers for inhibition assays in a 3-fold dilution, with a starting concentration of 50 nM or 100 nM, all concentrations of P-Tau are given in nM.*

Different P-Tau coating concentration in ng/ml	
100	10
Dilution series of P-Tau monomers in nM for inhibition assay	
50	100
16.7	33
5.6	11
1.9	3.7
0.6	1.2
0.2	0.4
0.07	0.1
0.0	0.0

3.8 Cross binding reaction and specificity was examined with pooled plasma samples using MSD competition assay

Examination of cross binding of anti-TDP-43 nAbs, anti-α-syn nAbs, and anti-Tau nAbs were done using the MSD competition assay. TDP-43 and α-syn are disease associated proteins associated with the pathology in ALS (Jeon et al., 2019) and MSA (Yamasaki et al., 2019), respectively. Both proteins cause similar to Tau brain pathology i.e. intracellular aggregates. TDP-43 (48.8 kDa) has a molecular weight similar to Tau (49.5 kDa) which is an important factor in the type of assays used here and makes the protein a good control. α-syn has a much lower molecular weight (14.4 kDa), however, it is a suitable disease control protein. It is important to mention that all proteinopathies are characterized by overlapping protein pathology (Spires-Jones et al., 2017).

From previous and ongoing studies at the Laboratory for Stereology and Neuroscience, the Bispebjerg-Frederiksberg Hospital, the concentrations of TDP-43 and α-syn for coating and inhibition used in control assays were selected. Plates were coated with 10 ng/ml Tau and pooled plasma samples from 10 PSP patients and 10 HCs were incubated in 1:200 dilution with an increasing concentration of either TDP-43 monomers [0-1000 nM], α-syn monomers [0-1000 nM], or Tau monomers [0-100 nM], all in a 3-fold dilution. TDP-43 and α-syn were first diluted a 10-fold and then diluted in 3-fold dilution. Furthermore, we examined pooled samples from 10 PSP, 10 MSA, and 10 ALS patients as well as 10 HCs on plates coated with 15 ng/ml of α-syn. The plasma pools were preincubated at 1:200 dilution with increasing concentrations of α-syn monomer [0-1000 nM].

3.9 Relative affinity/avidity of nAbs towards Tau or P-Tau in plasma samples from PSP patients and HCs in MSD competition assay

Day 1:

96-well microtiter plate (High bind MSD plate) were coated with 50 µl of 10 ng/ml recombinant Tau monomer or P-Tau monomer diluted in cold carbonate buffer overnight (>12h) at 4°C.

Day 2:

The plate was washed six times with 150 µl washing buffer (PBS + 0.05 % tween) and blocked for two hours on a shaker at 800 rpm at RT. The plate was washed six times with 150 µl washing buffer, and 25 µl of plasma (1:200 in PBS + 0.1 % BSA) were transferred to the plate and incubated one hour on a shaker at 800 rpm at RT. Before transferring the plasma to the plate, the individual samples were preincubated for one hour at RT with different concentration of Tau monomer or P-Tau monomer in a range of concentrations: 100 nM, 33 nM, 11 nM, 0.4 nM, 0.1 nM, and 0 nM for Tau or 50 nM, 5 nM, 1.7 nM, 0.6 nM, 0.2 nM, and 0 nM for P-Tau. The plate was washed six times with 150 µl washing buffer, and 25 µl MSD SULFO-TAG™, Goat Anti-Human IgG Antibody (1:500 diluted in PBS + 0.1% BSA) were transferred to each well and incubated for one hour on a shaker at 800 rpm at RT. The plate was washed six times with 150 µl washing buffer and finally 150 µl MSD Read Buffer T (4X) with Surfactant (1:2 diluted in distilled water) were transferred to the plate and read immediately afterwards using an MSD Sector Imager S600 instrument. A schematic overall set up of the experiment is shown in Figure 9.

Processing data obtained from the MSD Sector Imager S600; the percentage of max binding was calculated as followed:

$$\frac{ECL_X - ECL_{0\%\ binding\ (100\ nM\ Tau)}}{ECL_{100\ \%\ binding\ (0\ nM\ Tau)}} * 100\ \% = \%\ of\ \max binding$$

Where X being an arbitrary concentration of the Tau monomer or P-Tau monomer.

3.10 Enzyme-linked immunosorbent assay (ELISA)

ELISA is a technology where it is possible to detect and quantify different molecules, namely proteins in a relatively simple and not expensive way. ELISA assays are found in different formats and are typically performed in 96-well or 384-well (Overview of ELISA, Thermo Fisher Scientific). In this report, we are using the format indirect ELISA and 96-well plate.

3.10.1 Indirect ELISA

An antigen is captivated on the plate surface of the well, similar to MSD. Blocking buffer is used to saturate the unbound site left on the plate surface before adding primary Abs (e.g. Abs in plasma). A secondary Ab is subsequently added, typically the secondary Ab is conjugated with horseradish peroxidase (HRP). Another way to detect primary Ab (plasma Ab) is an addition of biotin conjugated Ab followed by detection with HRP conjugated to streptavidin (Figure 10). In case of both methods a substrate solution is then added to produce a colorimetric signal that is proportional to the amount of plasma Ab bound to the antigen on the plate (Enzyme Substrates for ELISA, Thermo Fisher Scientific; Overview of ELISA, Thermo Fisher Scientific).

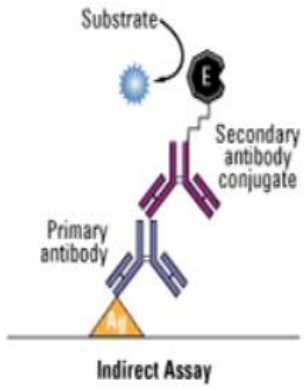

*Figure 10 | **Schematic overview of indirect ELISA.** An antigen is captivated on the plate surface which a primary antibody bind. A secondary antibody conjugated with e.g. horseradish peroxidase that can be detected with an enhanced colorimetric substrate. Figure from Enzyme Substrates for ELISA, Thermo Fisher Scientific; Overview of ELISA, Thermo Fisher Scientific.*

3.11 Optimization of indirect ELISA with pooled plasma samples from PSP patients and HCs; measuring the relative levels of IgG1-4 subclasses, total IgG, and IgM towards Tau using indirect ELISA

Optimizations for Tau ELISA were performed with pooled samples from 10 PSP patients and 10 HCs, before proceeding to the individual samples. Different coating concentrations of Tau, plasma dilutions, and antibody dilutions for IgG1-4 subclasses, IgM, and IgG total were tested, see table 6.

Table 6 | *Different coating concentrations of Tau, plasma dilutions, and antibody dilutions for IgG1-4 subclasses, total IgG, and IgM used in the optimization of indirect ELISA.*

Coating concentration of Tau	Plasma dilution	Antibody dilution	IgG1	IgG2	IgG3	IgG4
0.5 µg/ml	1:50		1:250	1:2000	1:200	1:100
0.1 µg/ml	1:100		1:500	1:4000	1:400	1:200
0.05 µg/ml	1:500		1:1000	1:5000	1:500	1:400
0.01 µg/ml	1:1000		1:2000	1:8000	1:1000	1:600
0.005 µg/ml			1:4000	1:10,000	1:2000	1:1000
				1:16,000	1:4000	1:2000
				1:32,000	1:8000	1:4000
						1:8000
			Total IgG	**IgM**		
			1:250	1:250		
			1:500	1:500		
			1:5000	1:2500		
			1:10,000	1:5000		
			1;20,000	1:10,000		

After the optimal coating concentration for Tau has been determined, the dilution series for the standard curve could be tested, see table 7. When examining the individual samples, each plate will have a column with a standard curve to account for plate to plate differences. Anti-total IgG was HRP conjugated where as anti-IgG1-4 and -IgM secondary Abs were biotin conjugated; thus, an additional step was required with Streptavidin conjugated to HRP. Therefore, two standard curves were needed.

Table 7 | *Dilution series of Anti-Tau HRP and Polyclonal Rabbit Anti-Human Tau for the standard curve.*

Anti-Tau HRP	1:100	1:200	1:400	1:800	1:1600	1:3200
Polyclonal Rabbit Anti-Human Tau	1:50,000	1:150,000	1:450,000	1:1,350,000	1:4,050,000	

3.12 Measurement of relative levels of IgG1-4 subclasses, total IgG, and IgM towards Tau using indirect ELISA

Day 1:

96-well Maxi Sorp plate were coated with 50 µl of 0.1 µg/ml or 0.05 µg/ml recombinant Tau monomer diluted in cold carbonate buffer and incubated overnight (>12h) at 4°C.

Day 2:

The plate was washed three times with 300 µl washing buffer (PBS + 0.1 % tween) in the WellWash machine, for a more consistent wash, and blocked with blocking buffer (PBS + 3% BSA) for two hours at RT. The plate was washed three times with 300 µl washing buffer, and then 50 µl of plasma (1:100 (IgG1-4), 1:500 (IgM), and 1:1000 (total IgG) in PBS + 0.1 % BSA) was transferred to the plate and incubated for one hour at RT. The plate was washed three times with 300 µl washing buffer, and 50 µl of diluted anti-IgG1 (1:2000), -IgG2 (1:5000), -IgG3 (1:400), -IgG4 (1:600), -total IgG (1:10,000) or -IgM (1:250) were transferred to the plate and incubated for one hour at RT. Anti-IgG1 was transferred to the plate coated with 0.1 µg/ml and anti-IgG2-4 subclasses, -total IgG, and -IgM were transferred on 0.05 µg/ml coating. The plate was washed three times with 300 µl washing buffer. Streptavidin-Peroxidase was added to the plate and incubated for 30 min at RT. Fifty µl of TMB ONE was transferred to the plate and incubated for 30 min in the dark at RT. Prior use, TMB ONE was heated to RT in darkness. After addition of TMB ONE, 50 µl 0.5 % H_2SO_4 were transferred to the plate and the plate was read at 450 nm in the ELISA plate reader.

For each plate a standard curve was made to ensure all results were normalized as well as accounted for the differences on the plates. Fifty µl of polyclonal Rabbit Anti-Human Tau or Anti-Human Tau HRP were transferred to one row of the plate in a range of 1:25,000-

1:18,225,000 in a 3-fold dilution or 1:50,000-1:36,450,000 in a 3-fold dilution, respectively. The standard curves for anti-IgG1-4 and -IgM, 50 µl of biotinylated Goat Anti-Rabbit IgGs were added and incubated for 30 min at RT. The plate was washed three times with 300 µl washing buffer, and then 50 µl Streptavidin-Peroxidase was transferred to each well. The standard curve for total IgG, 50 µl of HRP Anti-Human Tau was added and incubated for one hour at RT. The plate was then washed three times with 300 µl washing buffer.

3.13 Quantification of global levels of IgG1-4 subclasses, total IgG, and IgM in PSP patients and HCs using indirect ELISA kits

Specific ELISA kits were purchased for measuring of global IgG1 (Cat. No. 88-50560-22, Thermo Fisher Scientific), IgG2 (Cat. No. 88-50570-22, Thermo Fisher Scientific), IgG3 (Cat. No. 88-50580-22, Thermo Fisher Scientific), IgG4 (Cat. No. 88-50590-22, Thermo Fisher Scientific), total IgG (Cat. No. 88-50550-88, Thermo Fisher Scientific), and IgM (Cat. No. 88-50620-88, Thermo Fisher Scientific). The protocols were followed as suggested by the manufacturer, with only few changes.

Day 1:

Corning™ Costar™ 9018 96-well ELISA plate or 96-well Maxi Sorp plate were coated with 100 µl 1:250 dilution of the proper capture Ab in cold Coating Buffer overnight (>12h) at 4°C. Corning™ Costar™ 9018 96-well ELISA plate was used for IgG1-4 subclasses and IgM, and 96-well Maxi Sorp plate was used for total IgG.

Day 2:

The plate was washed two times with 400 µl washing buffer (PBS + 0.1 % tween) and 1-minute soak each time in the WellWash machine, and blocked with Blocking Buffer for two hours at RT. The plate was washed two times with 400 µl washing buffer and 1-minute soak each time, and then 100 µl of plasma diluted in Assay Buffer A (IgG1 prediluted plasma 1:2000 ; IgG2 prediluted plasma 1:500,000 ; IgG3 prediluted plasma 1:40,000 ; IgG4 prediluted plasma 1:50,000 ; total IgG prediluted plasma 1:500,000 ; IgM prediluted plasma 1:20,000) was transferred to the plate and incubated two hours at RT. All individual plasma samples were made in the proper dilution the day before and stored at 4°C. The plate was washed two times with 400 µl washing buffer and 1-minute soak each time, and 100 µl 1:250 of proper diluted detection Ab were added to the plate and incubated for one hour at RT. The plate was washed two times with 400 µl washing buffer and 1-minute soak each time and 100 µl Substrate

solution was transferred to the plate and incubated for 15 min in the dark at RT. Prior use, Substrate solution was heated to RT in darkness. After addition of Substrate solution, 100 µl of 0.5 % H_2SO_4 were transferred to the plate and the plate were read at 450 nm using the ELISA plate reader.

For each kit a standard curve dilution series were made according to the manufacturer's protocol and 100 µl of each dilution were transferred to appropriate well on each plate. The standard curve was later used to estimate the absolute concentration of a given Ab (mg/dl) for each sample.

3.14 Statistical analyses

All statistical analyses of the data were performed in GraphPad Prism 8.0.0 software program. Demographic differences of age and gender were analysed by an unpaired Student's t test and chi-square, respectively. The two-site inhibition curves were made in GraphPad using Two sites - Fit logIC50. The ROUT method was used to remove outliers from the analysed data. All data were verified for normal distribution before using the Student's t test, and if the data were not normally distributed the data were transformed to Log10 logarithm scale. The Student's t test was used for statistical comparison. Nonetheless if the data were not normally distributed or lognormal distributed the Mann Whitney test was used to analyse for any differences in the samples. Statistical difference was accepted with a P-value < 0.05. Spearman's test was used to investigate for correlation between collected data and Hoehn & Yahr disease stage scale or disease duration.

4. Results

4.1 Optimization steps; relative affinity/avidity of nAbs towards Tau in pooled plasma samples from PSP patients and HCs in MSD competition assay

To optimize the respective conditions for MSD competition assay, we tested plasma pools in different dilutions, plate coating concentrations, as well as various blocking buffers. Subsequently, Tau concentrations for the inhibition assay were determined. Figure 11 presents results from the initial experiments. To define the optimal working dilutions of coating protein and plasma, several titrations of plasma pools and coating protein were prepared and assayed simultaneously on MULTI-ARRAY standard MSD plate (Figure 11A). The binding index obtained with 1:200 plasma dilution (Figure 11A, black) was more consistent in comparison to 1:500 (Figure 11A, red) and 1:1000 plasma dilutions (Figure 11A, green) on the wells coated with increasing concentration of Tau. The binding index increased with the higher coating, however, with coating >50 ng/ml of Tau the binding index reached plateau and started to decrease. There were no major differences in binding indices between wells coated with 10 ng/ml and 50 ng/ml of Tau (Figure 11A, black white-circles) suggesting these two being the optimal coating. Wells coated with > 50 ng/ml of Tau showed a decreasing binding index, which could suggest saturation of Ab binding or Tau aggregation due to the high concentration of the protein.

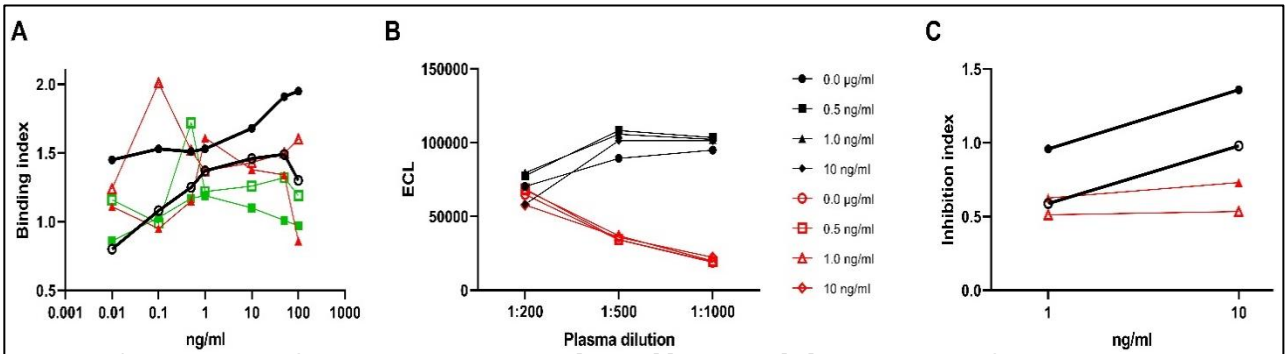

Figure 11 | ***Optimization of coating concentrations, plasma dilutions and plate comparison for MSD competition assay.*** *Different coating concentrations and pooled plasma dilutions were examined* ***A.*** *presents the binding index of different plasma dilutions on different coating concentrations on standard MSD plate; 1:200 plasma dilution (black, PSP-circle, HC-white circle), 1:500 plasma dilution (red, PSP-square, HC-white square), and 1:1000 plasma dilution (green, PSP-triangle, HC-white triangle).* ***B.*** *presents a comparison between using standard MSD plate (red lines) and high bind MSD plate (black lines). Different plasma dilutions were examined on different coating concentrations and plates were blocked with SuperBlock buffer.* ***C.*** *presents inhibition index for comparison of different coating concentrations and plasma dilutions; 1:200 plasma dilution (black, PSP-circle, HC-white circle) and 1:500 plasma dilution (red, PSP-triangle, HC-white triangle).*

MSD provides plates with two surface types: High Bind plates having a hydrophilic surface, and Standard plates having a hydrophobic surface. Therefore, a combination of working electrode

size and surface type determines the capacity to capture protein that can be coated on the plate. Figure 11B shows a comparison of standard MSD plate (red) and high bind MSD plate (black) coated with several Tau dilutions (0.5-10 ng/ml). Despite decreasing plasma dilution, the high bind plate provided an increasing ECL signal but a decreasing ECL signal was observed using the standard plate. Thus, high bind MSD plates were chosen for further experiments. In the initial optimization setups, a standard blocking buffer PBS + 3% BSA was used, however, based on tests with different blocking buffers, we exchanged to SuperBlock buffer, as a better signal to noise was achieved. Comparing the results when using blocking buffer PBS + 3% BSA or SuperBlock buffer, the latter showed superior sensitivity. The high bind plate showed a better capacity of capturing Tau, which is indicated by the higher ECL signal (Figure 11B).

To further optimize the optimal coating and plasma dilutions, we proceeded to the inhibition assay. Figure 11C shows the inhibition index for plasma incubated with 100 nM Tau monomer or with dilution buffer, on high bind MSD plate coated with 1 ng/ml and 10 ng/ml. The inhibition index increased for 1:200 plasma dilution (black lines) from 1 ng/ml to 10 ng/ml coating, however with 1:500 plasma dilution it almost remained on the same level.

Figure 12 presents examples of a two-site inhibition curves, obtained during optimization of MSD competition assay. The y-axis represents percentage of maximum binding, which indicates an occupation of anti-Tau nAbs by different concentration of the antigen in fluid phase. The x-axis represents increasing concentration of free Tau monomers in nM, transformed to a logarithmic (Log10) scale. High affinity nAbs are characterized by efficient inhibition of Tau binding, when a low concentration of free Tau monomers was present (0.1 – 0.4 nM) in the fluid phase, whereas low affinity nAbs were efficiently inhibited by free Tau monomers at high concentrations (11 – 33.3 nM) in the fluid phase. Hence, Figure 12C indicates that 50 % in the two-site inhibition curve defines efficient inhibition; above 50 % defines high affinity/avidity nAbs whereas below 50 % defines low affinity/avidity nAbs.

The purpose for using the two-site inhibition curve was to observe distinct differences in the Tau affinity profiles in the plasma sample from the two groups. Figure 12A and C shows a distinct difference in Tau affinity profile when wells were coated with 10 ng/ml of Tau and 1:200 plasma samples of PSP patients (red line) and HCs (black line) were preincubated with increasing Tau concentration in the fluid phase. HCs (black line) showed a decreasing Ab

binding present in low concentrations [0.2-11 nM] of Tau monomers, suggesting approximately 50 % of the total Ab binding are high affinity/avidity Ab. However, this was not observed for PSP patients (red line) where sufficient inhibition was observed only with high concentrations of Tau [11-33 nM]. However, using pooled plasma samples diluted 1:500 show no distinct differences and sufficient plasma inhibition was only observed with high concentrations of Tau [11-33 nM] for both groups (Figure 12B). Coating the wells with 1 ng/ml of Tau, the results were unclear due to inconsistency in the data (Figure 12D).

For the experiments examining individual samples, high bind MSD plates were coated with 10 ng/ml of Tau, and 1:200 diluted plasma was preincubated with a concentration range of 0-100 nM of free Tau monomers.

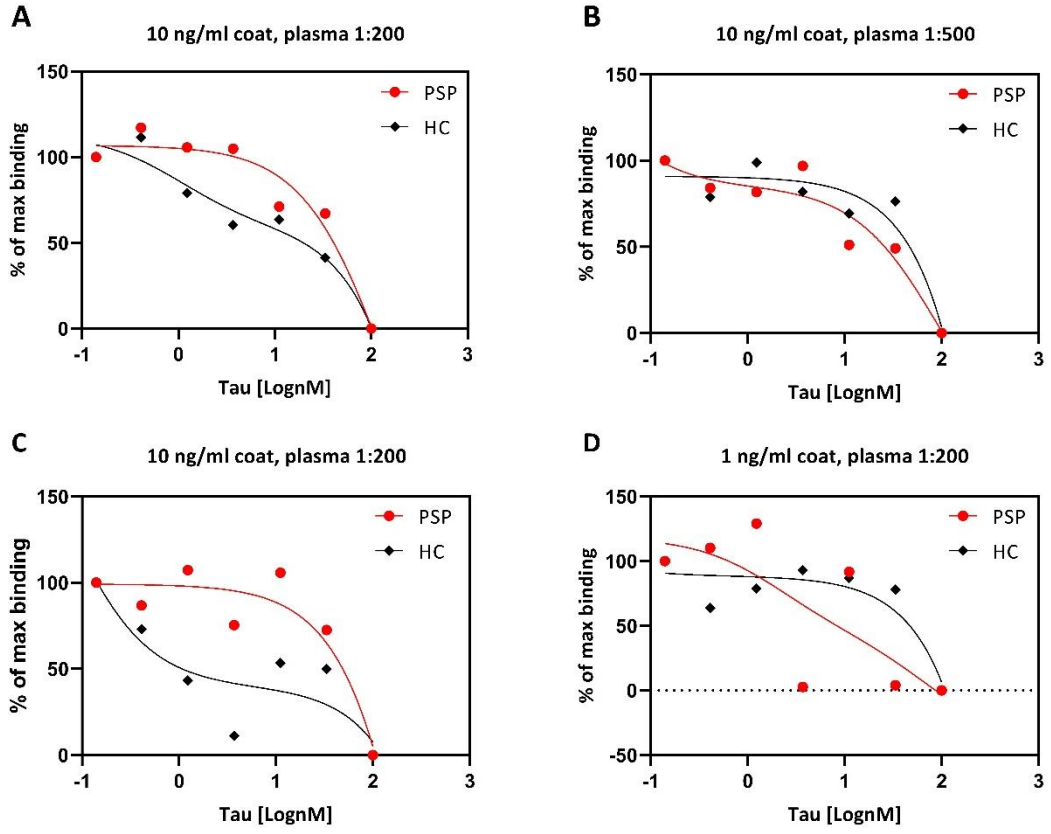

*Figure 12 | **MSD competition assay with Tau on high bind MSD plate – two-site inhibition curves.** Pooled samples from PSP patients (red) (n=10) and HCs (black) (n=10). **A.** 10 ng/ml are coated on the plate and the plasma dilution is 1:200. **B.** 10 ng/ml are coated on the plate and the plasma dilution is 1:500. **C.** 10 ng/ml are coated on the plate and the plasma dilution is 1:200. **D.** 1 ng/ml are coated on the plate and the plasma dilution is 1:200.*

4.2 Optimization steps; relative affinity/avidity of nAbs towards phosphorylated Tau in pooled plasma samples from PSP patients and HCs in MSD competition assay

Abnormal P-Tau forming NTFs has been observed in both PSP and AD (Dickson et al., 2007; Spires-Jones et al., 2017). Therefore, in addition to measuring nAbs affinity/avidity towards Tau, we decided to examine nAbs affinity/avidity towards P-Tau. Before examining individual plasma samples from PSP patients and HCs, the competition conditions had to be optimized to find the optimal coating concentration and P-Tau concentration for the inhibition assay. Based on the previous experiments with Tau, the different concentrations of P-Tau were preselected. The plasma concentration was kept 1:200 similarly to previous assays to maintain consistency and make the results comparable. Figure 13 shows the two-site inhibition curves with different coating concentrations and P-Tau concentrations used in the inhibition assays. As seen in Figure 13A and B, the high bind MSD plates were coated with 100 ng/ml of P-Tau and pooled plasma samples were preincubated with two concentration range of free P-Tau monomers [0-100 nM] and [0.1-33 nM]. No discrepancies in the inhibition profiles between the groups were observed, thus it was decided to coat the plates with a lower P-Tau concentration, 10 ng/ml, and preincubated pooled plasma with three concentration range of free P-Tau monomers [0-

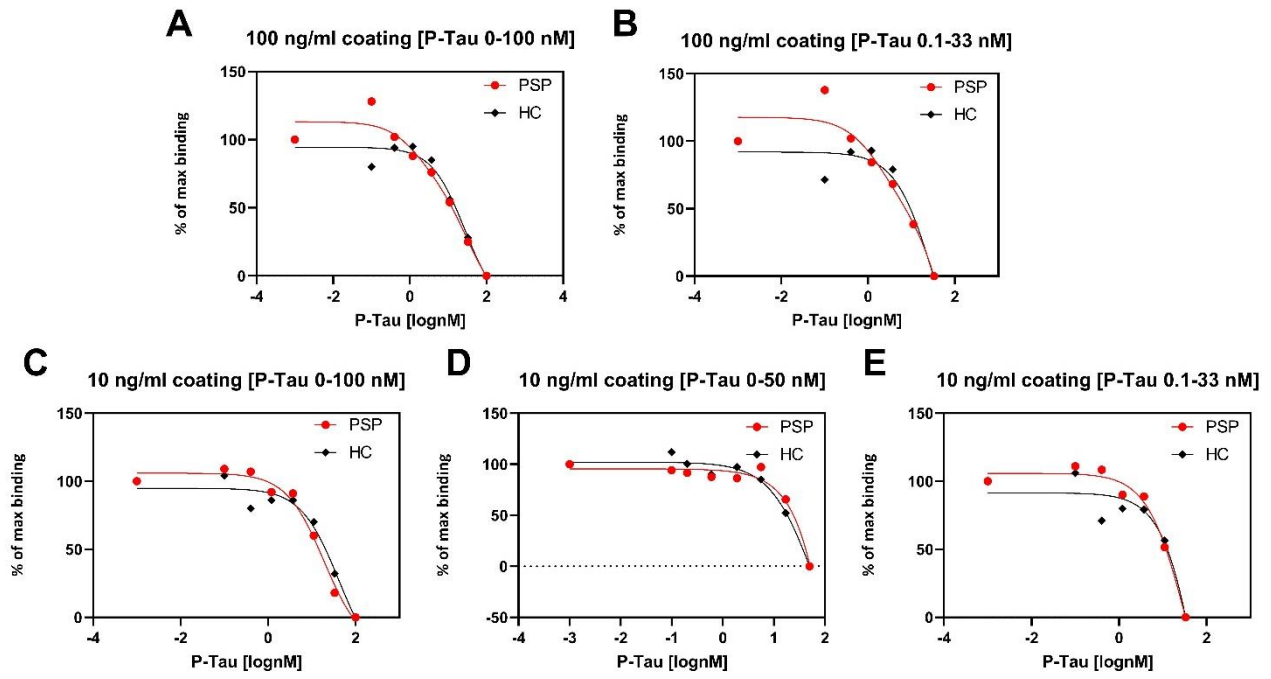

*Figure 13 | **MSD competition assay with P-Tau– two site inhibition curves.** Pooled samples from PSP patients (red) (n=10) and HCs (black) (n=10). The graphs in **A.** and **B.** were coated with 100 ng/ml of P-Tau and the concentration range for the inhibition assay of P-Tau monomers were [0-100 nM] and [0.1-33 nM]. The graphs in **C.**, **D.**, and **E.** were coated with 10 ng/ml of P-Tau and the concentration range for the inhibition assay of P-Tau monomers were [0-100 nM], [0-50 nM], and [0.1-33 nM].*

100 nM], [0-50 nM], and [0.1-33 nM] (Figure 13C, D, and E). We did not observe differences between the affinity profiles.

The initial experiments with pooled plasma samples indicating no differences in the apparent affinity/avidity of anti-P-Tau profiles in PSP patients and HCs. Based on that we selected 10 ng/ml of P-Tau to coat the plates and, the concentration range of P-Tau monomers [0-50 nM] for the inhibition assays were chosen for experiments with individual samples.

4.3 MSD competition assay; relative affinity/avidity of nAbs towards Tau and P-Tau in individual plasma samples from PSP patients and HCs

Using optimized MSD competition assay it has been possible to quantify the apparent affinity/avidity of anti-Tau nAbs in the individual plasma samples from 55 PSP patients and 59 HCs. Figure 14 shows the percentage of maximum binding of anti-Tau nAbs per individual (y-axis) for each group, PSP patients and HCs (x-axis). Each plasma sample was diluted 1:200 with PBS and preincubated with a low [0.1-11 nM] and high [33-100 nM] concentration range of Tau monomers, followed by incubation on precoated plate with 10 ng/ml of immobilized Tau. In the presence of 0.4 nM Tau monomers data show approximately 85-95 % and 75-85 % of maximum binding of anti-Tau nAbs obtained in plasma samples from PSP patients and HCs, respectively (Figure 14A). In the presence of 11 nM Tau monomers data show approximately 75-85 % and 65-70 % of maximum binding of anti-Tau nAbs obtained in plasma samples from PSP patients and HCs, respectively (Figure 14B). Under these conditions PSP patients were significantly different from HCs, suggesting that the patients have a significantly lower amounts of high affinity anti-Tau nAbs in plasma compared to controls. In the presence of 0.1 nM Tau monomers data show approximately 85-95 % and 80-90 % of maximum binding of anti-Tau nAbs obtained in plasma samples from PSP patients and HCs, respectively (Figure 14A). Data show approximately 55-65 % and 50-60 % of maximum binding of anti-Tau nAbs obtained in plasma samples from PSP patients and HCs, respectively, in the presence of 33 nM Tau monomers (Figure 14D). No statistical differences were observed for 0.1 nM and 33 nM concentrations of free Tau monomers.

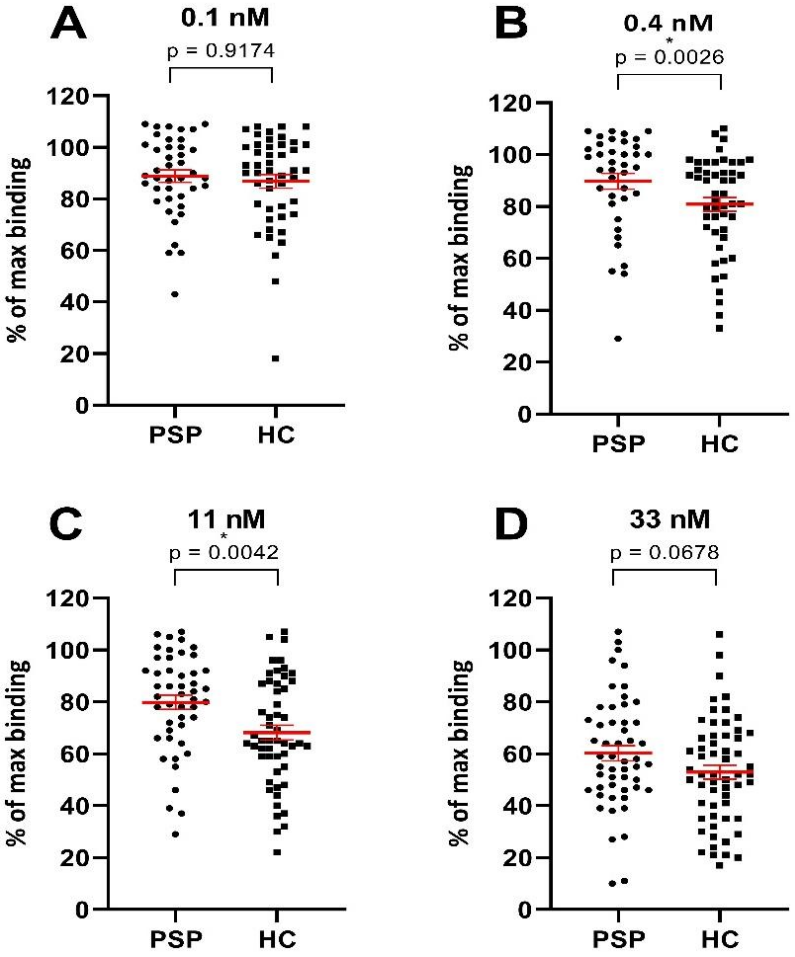

*Figure 14 | **Affinity/avidity measured in individual plasma samples.** MSD competition assay quantifying the affinity/avidity of anti-Tau nAbs towards Tau in individual plasma samples from PSP patients and HCs. Different concentrations of Tau monomers were used in the inhibition of anti-Tau nAbs in each assay; **A.** 0.1 nM Tau, **B.** 0.4 nM Tau, **C.** 11 nM Tau, and **D.** 33 nM Tau. The absence of free Tau monomer (0 nM) is defining maximal binding of anti-Tau nAbs to the immobilized Tau, and non-specific binding to the plate is observed with the highest concentration of free Tau monomers (100 nM). All data points under 0 % and over 110 % were removed from the analysis. Horizontal bars (red) represent the mean values +/- SEM. Significance was tested using Student's test or Mann Whitney test, depending on the data were normalized or not. * indicates significant difference.*

Figure 15 shows the percentage of maximum binding of anti-P-Tau nAbs per individual (y-axis) for each group, PSP patients or HCs (x-axis). Each plasma sample was diluted 1:200 with PBS and preincubated with low [0.2-1.7 nM] and high [5-50 nM] concentrations of P-Tau monomers, followed by incubation on precoated plate with 10 ng/ml of immobilized P-Tau. In the presence of 0.6 nM P-Tau monomers data show approximately 90-95 % and 85-90 % of maximum binding of anti-P-Tau nAbs obtained in plasma samples from PSP patients and HCs, respectively (Figure 15B). The corresponding value for HCs is significantly lower in comparison with PSP patients, indicating increased levels of affinity/avidity anti-P-Tau nAbs in HCs. The maximum binding of anti-P-Tau nAbs obtained in plasma samples from PSP patients and HCs in the presence of 0.2 nM P-Tau monomers was approximately 85-95 % and 90-95 %, respectively (Figure 15A). In the presence of 1.7 nM P-Tau monomers, data show approximately 80-90 % and 80-85 % of maximum binding of anti-P-Tau nAbs obtained in plasma samples from PSP patients and HCs, respectively (Figure 15C). In the presence of 5 nM P-Tau monomers data

show approximately 75-80 % and 75-80 % of maximum binding of anti-P-Tau nAbs obtained in plasma samples from PSP patients and HCs, respectively (Figure 15D). No statistical differences between the groups was observed for 0.2 nM, 1.7 nM, and 5 nM concentrations of free P-Tau monomers.

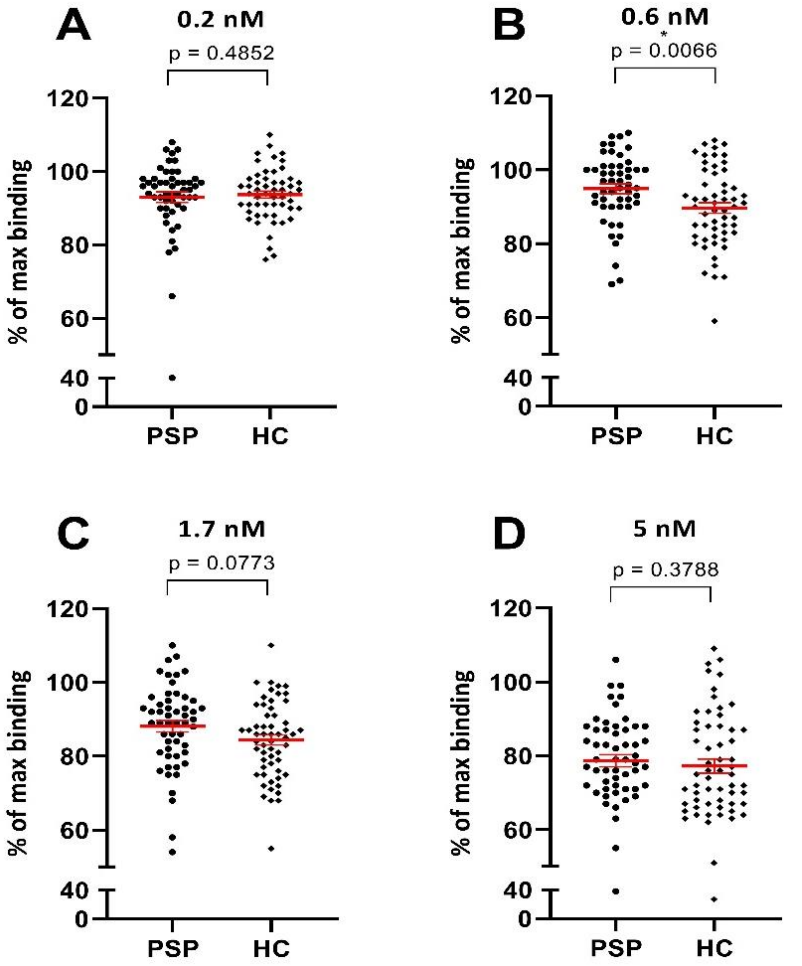

*Figure 15 | **Affinity/avidity measured in individual plasma samples.** MSD competition assay quantifying the affinity/avidity of anti-P-Tau nAbs towards P-Tau in plasma samples from PSP patients and HCs. Different concentrations of P-Tau monomers were used in the inhibition of anti-P-Tau nAbs in each assay; **A.** 0.2 nM P-Tau, **B.** 0.6 nM P-Tau, **C.** 1.7 nM P-Tau, and **D.** 5 nM P-Tau. The absence of free P-Tau monomer (0 nM) is defining maximal binding of anti-P-Tau nAbs to the immobilized P-Tau, and non-specific binding to the plate is observed with the highest concentration of free P-Tau monomers (50 nM). All data points under 0 % and over 110 % were removed from the analysis. Horizontal bars (red) represent the mean values +/- SEM. Significance was tested using Student's test or Mann Whitney test, depending on the data were normalized or not. * indicates significant difference.*

Following, we checked if there was any correlation between the measured affinity/avidity of anti-Tau nAbs or anti-P-Tau nAbs and either the disease duration or scores on the Hoehn & Yahr scale. No correlations were seen, see appendix 2 and 3.

4.4 Binding properties of anti-TDP-43 nAbs, anti-α-synuclein nAbs, and anti-Tau nAbs towards TDP-43, α-synuclein, and Tau in pooled plasma samples

In addition to measuring affinity/avidity of anti-Tau nAbs towards Tau, we wanted to ensure there was no cross reaction to other disease associated proteins, TDP-43 and α-syn. The aim was to conduct a control competition assays to evaluate anti-Tau nAbs specificity as well as

evaluate if nAbs are epitope specific. Therefore, we used the competition assay on MSD platform to examine if there were any cross protein reaction between anti-α-syn, anti-TDP-43, or anti-Tau nAbs in pooled plasma samples from PSP patients and HCs. (Albus et al., 2018; Spires-Jones et al., 2017).

Pooled plasma samples were diluted 1:200 with PBS and preincubated with TDP-43 [0-1000 nM], α-syn [0-1000 nM], or Tau [0-100 nM] monomers, followed by incubation on precoated high bind MSD plate with 10 ng/ml of immobilized Tau. Tau monomers were able to inhibit anti-Tau nAbs binding to the plate in PSP patients and HCs (Figure 16, green lines), however both TDP-43 (Figure 16, black circles) and α-syn (Figure 16, red squares) did not show an inhibition of anti-Tau nAbs binding expressed as % of inhibition. Antibody/antigen complexes for TDP-43 and α-syn are washed off during the washing procedure revealing that only anti-Tau nAbs binds to the immobilized Tau on the bottom, suggesting no cross reaction (Figure 16).

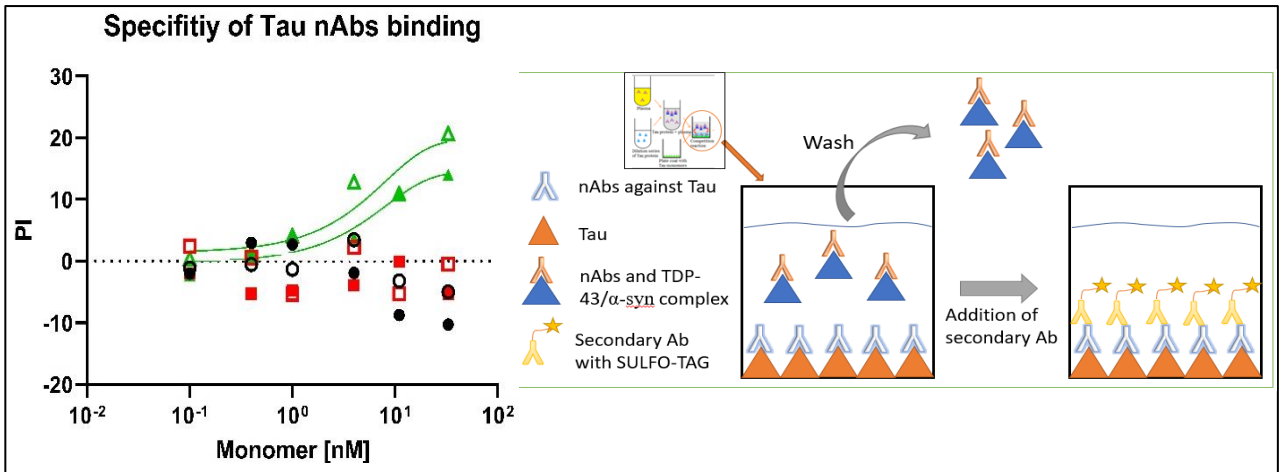

Figure 16 | ***Specificity binding of anti-Tau nAbs and schematic overview of competition reaction.*** *Data is presented as % of inhibition (PI) relative to unblocked condition; unblocked condition = 0 nM monomers. The plate is coated with 10 ng/ml Tau and the competition reaction is performed with monomers of TDP-43 [0-1000 nM] (black PSP-circle, HC- white circle), α-syn [0-1000 nM] (red, PSP-square, HC-white square), or Tau [0-100 nM] (green, PSP-triangle, HC-white triangle). Schematic overview of the competition reaction (see Figure 9) when coating with Tau and using TDP-43 or α-syn for competition, showing no cross reaction of the nAbs. Secondary Abs conjugated with SULFO-TAG are interacting with the nAbs bound to the immobilized Tau and is then measured through the emitted light.*

Neurodegenerative diseases are characterized by protein aggregation presented very often with mixed pathology (Moussaud et al., 2014; Spires-Jones et al., 2017). We have evaluated relative binding properties of anti-α-syn nAbs in plasma samples from MSA, ALS, PSP patients in comparison with HCs. High bind MSD plates were coated with 15 ng/ml of α-syn and pooled plasma samples were preincubated with increasing concentrations of α-syn [0-1000 nM]. The inhibition curve distinctly follows a two-site model for plasma samples from ALS patients and

HCs, indicating that a substantial fraction of total Ab binding is characterized by high affinity/avidity nAbs, approximately 50 %. However, the pooled plasma samples from MSA and PSP patients needed high α-syn concentrations [>33 nM] for efficient inhibition, indicating an absence of high affinity/avidity nAbs (Figure 17).

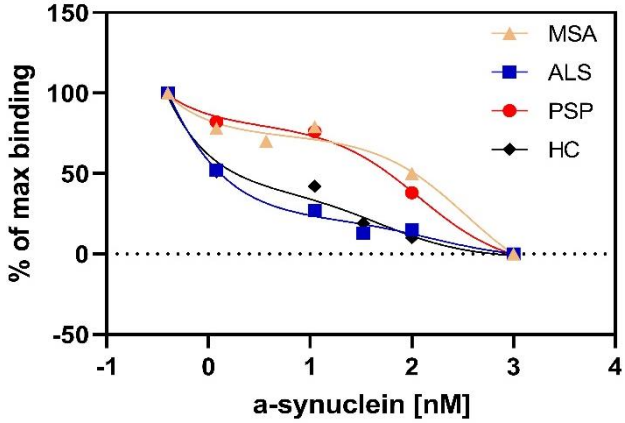

Figure 17 | ***Two-site inhibition curve of cross reaction.*** *Pooled plasma samples from MSA (complexion), ALS (purple), PSP (green) patients, and HCs (bla.ck) were diluted 1:200 in PBS and preincubated with α-syn [0-1000 nM] and then incubated on a precoated high bind MSD plate with 15 ng/ml of α-syn. The y-axis shows the % of maximum binding, which indicates an occupation of all anti-α-syn NAbs and x-axis show the concentration of α-syn [nM]. The absence of free α-syn monomer (0 nM) is defining maximal binding of anti-α-syn nAbs to the immobilized α-syn, and non-specific binding to the plate is observed with the highest concentration of free α-syn monomers (1000 nM).*

4.5 Optimization steps; measurement of relative levels of IgG1-4 subclasses, total IgG, and IgM towards Tau in pooled plasma samples from PSP patients and HCs using indirect ELISA

Following, we aimed to investigate the relative levels of IgG1-4 subclasses, total IgG, IgM specific for Tau in the individual plasma samples from PSP patients and HCs using indirect ELISA. Before examining individual samples from PSP patients and HCs, optimization of indirect ELISA was performed on plasma pools to determine a proper plasma dilution, coating concentration, and secondary Ab dilutions. Throughout the optimization we encountered difficulties with the secondary Abs, due to high background signals, which probably was a result of an unspecific binding of the secondary Ab to the plate. Therefore, different secondary Abs were examined together with several blocking and dilution buffers, see appendix 4.

The selected secondary Abs from Merck (Sigma-Aldrich) (Anti-IgG2-4 and anti-IgM), Abcam (Anti-total IgG), and Invitrogen (Anti-IgG1) were optimized before examining individual samples. Figure 18 presents the absorbance (OD_{450}) on the y-axis and secondary Ab dilutions on the x-axis. Plates were coated with different concentrations of Tau 0.1 ng/ml (red), 0.05 ng/ml (blue), and 0.01 ng/ml (green), and plates were incubated with 1:100 (Figure 18A-D), 1:500 Figure 18F), or 1:1000 (Figure 18E) pooled plasma samples (circle, triangle, and square) and dilution buffer (white-circle, white-triangle, and white-square). A clear difference is seen

between the use of plasma dilution and dilution buffer; however, the different coating concentration did not have any significant effect on the Ab dilution.

However, more unspecific binding to the plate was observed with anti-IgG1 Abs; thus, we coated the plate with 0.1 ng/ml for IgG1, because higher binding indices between the plasma and dilution buffer were observed. 0.05 ng/ml coating was selected for anti-IgG2-4, anti-total IgG, and anti-IgM. Plasma was dilution 1:100, 1:500, and 1:1000 for anti-IgG1-4 subclasses, anti-IgM, and anti-total IgG, respectively. Based on data presented in Figure 18 we selected secondary Ab dilution as follows: anti-IgG1 diluted 1:2000, anti-IgG2 diluted 1:5000, anti-IgG3 diluted 1:400, anti-IgG4 diluted 1:600, anti-total IgG diluted 1:10,000, and anti-IgM diluted 1:250.

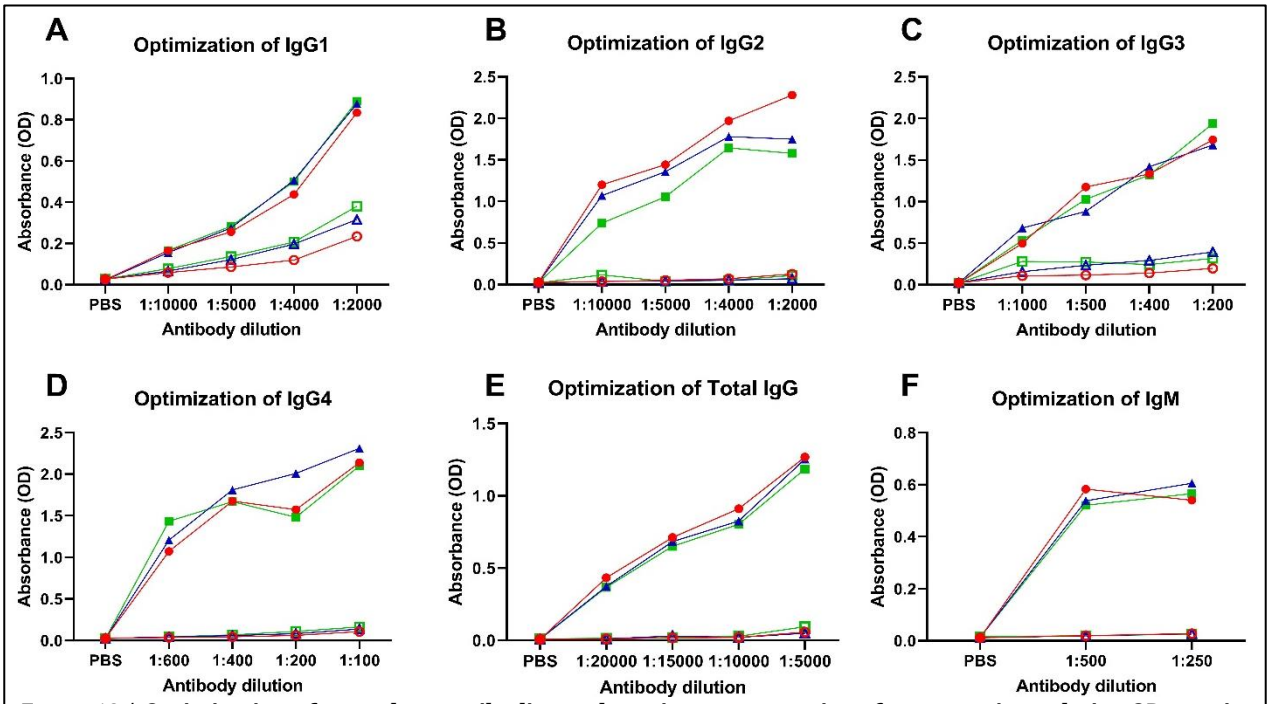

Figure 18 | ***Optimization of secondary antibodies and coating concentrations for measuring relative OD_{450} using indirect ELISA.*** *The antibody serial dilution for anti-IgG1-4 subclasses, anti-total IgG, and anti-IgM were chosen from either earlier experiment performed at the laboratory or the manufacture's recommendation. Y-axis shows the absorbance in OD and x-axis shows the antibody dilutions. Plasma dilutions (Circle, triangle, and square) and dilution buffer (white-circle, white-triangle, and white-square) were incubated on 96-well Maxi sorp plate coated with 0.1 µg/ml Tau (red), 0.05 µg/ml Tau (blue), or 0.01 µg/ml Tau (green).* ***A-D.*** *1:100 plasma dilution was used with anti-IgG1-4,* ***F.*** *1:500 plasma dilution was used with anti-IgM, and* ***E.*** *1:1000 plasma dilution was used with anti-total IgG*

4.6 Measurement of relative levels of IgG1-4 subclasses, total IgG, and IgM towards Tau in individual plasma samples from PSP patients and HCs using indirect ELISA

To measure relative concentrations of anti-Tau IgG1-4 subclasses, total IgG, and IgM in the individual plasma samples, previously optimized indirect ELISA assays were used. Plates were coated with 0.1 ng/ml of Tau for anti-IgG1 and 0.05 ng/ml of Tau for anti-IgG2-4 subclasses, anti-total IgG, and anti-IgM. Individual plasma samples were diluted in PBS + 0.1 % BSA; 1:200 for anti-IgG1-4 subclasses, 1:500 for anti-IgM, and 1:1000 for anti-total IgG. The secondary Abs were diluted in PBS + 0.1 % BSA as follows: anti-IgG1 diluted 1:2000, anti-IgG2 diluted 1:5000, anti-IgG3 diluted 1:400, anti-IgG4 diluted 1:600, anti-total IgG diluted 1:10,000, and anti-IgM diluted 1:250. We observed significant difference in levels of anti-Tau IgG1, showing a higher

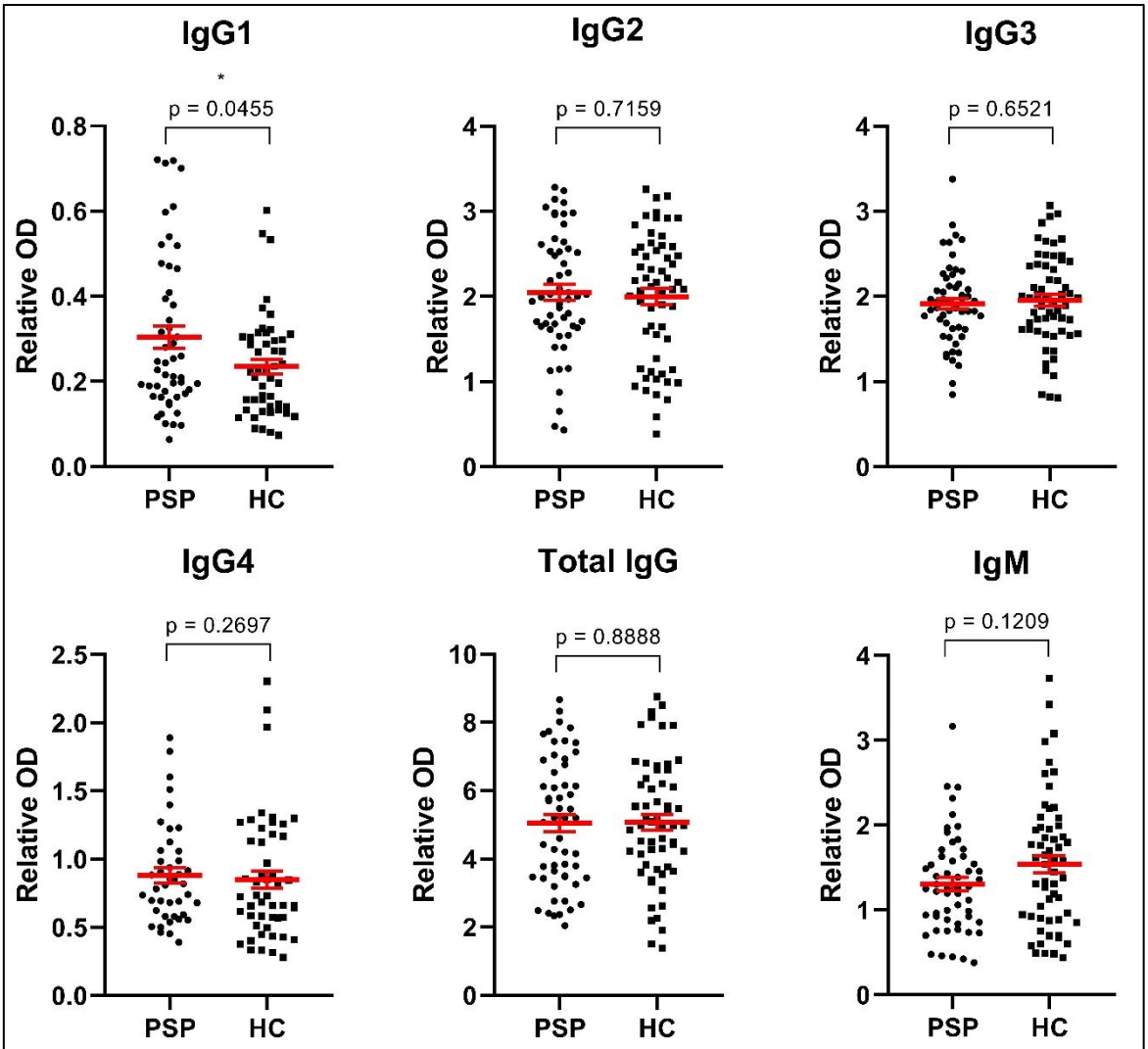

Figure 19 | ***Measurement of relative levels of anti-Tau IgG1-4 subclasses, total IgG, and IgM.*** *Y-axis shows the relative OD measured for each individual sample from PSP patients and HCs (x-axis). The average of standard curve for each plate was divided with the measured OD for all individual samples to calculate the relative OD. There was no significant difference between the tested groups, expect for IgG1 which it seems the group for PSP patients have a higher relative OD compared to HCs. All p-values are shown for each Ig; * indicates significant difference.*

relative levels of anti-Tau IgG1 in PSP patients in comparison with HCs. We found no significant difference in the relative levels of anti-Tau IgG2-4 subclasses, total IgG, and IgM in PSP patients and HCs (Figure 19).

Following, we checked if there was any correlation between the relative levels of anti-Tau IgG1-4 subclasses, total IgG, and IgM and either the disease duration or scores on the Hoehn & Yahr scale. No correlations were seen, see appendix 5.

4.7 Measurement of global levels of IgG1-4 subclasses, total IgGs, and IgMs in individual plasma samples PSP patients and HCs using indirect ELISA kits

In addition to measuring the relative levels of anti-Tau nAbs, it was of interest to investigate the global (overall) levels of IgG1-4 subclasses, total IgGs, and IgMs. Using commercially

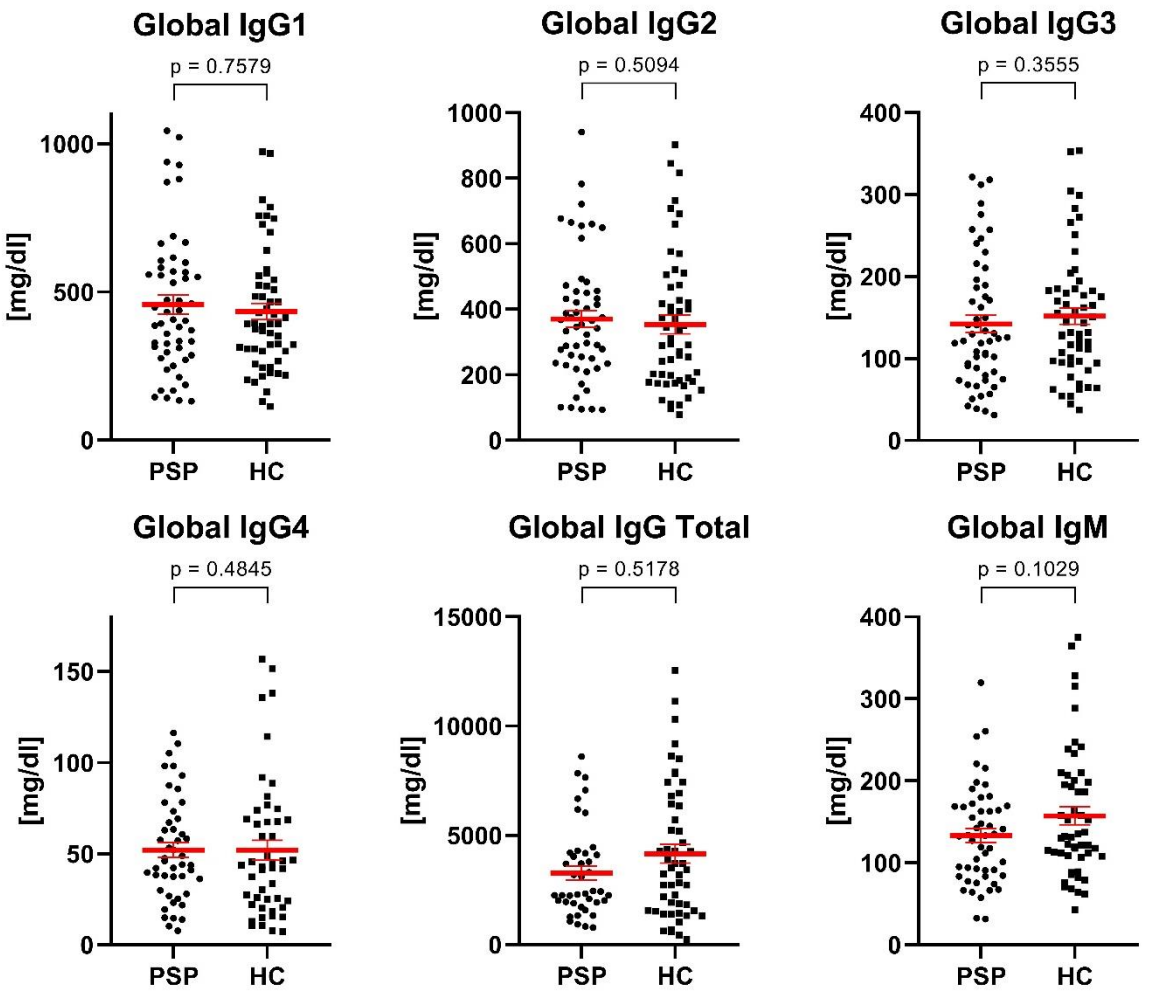

Figure 20 | ***Measurement of global IgG1-4 subclasses, total IgG, and IgM.*** *Y-axis shows the mg/dl calculated for each individual sample from PSP patients and HCs (x-axis). ELISA kits for each Ig was used to examine the global Ig in all individual samples. Each plate had a standard curve with a known concentration, which was made according the manufactures protocol. From this it was possible to calculate the Ig concentration in mg/dl, when taking the dilution factors into account. No significant differences were observed in global levels of Igs.*

available ELISA kits from Thermo Fisher Scientific it was possible to determine the precise concentrations (mg/dl) of Abs in the individual plasma samples from PSP patients and HCs. Plates were coated with the proper capture Ab diluted 1:250 in Coating buffer and plasma samples were differently diluted in Assay Buffer A according to the Ig; diluted plasma 1:2000 for IgG1, diluted plasma 1:500,000 for IgG2, diluted plasma 1:40,000 for IgG3, diluted plasma 1:50,000 for IgG4, diluted plasma 1:500,000 for total IgG, diluted plasma 1:20,000 for IgM. All secondary Abs were diluted 1:250 in Assay Buffer A. The global levels IgG1-4 subclasses, total IgG, and IgM were similar for PSP patients and HCs (Figure 20).

Furthermore, we investigated whether there was any correlation between the global levels for IgG1-4 subclasses, total IgGs, and IgMs and either the disease duration or scores on the Hoehn & Yahr scale. No correlations were seen, see appendix 6.

5. Discussion

Alteration in affinity/avidity nAbs and levels of Igs have previously been investigated in several neurodegenerative disorders including AD, PD, and ALS. To our knowledge this is the first study to investigate affinity/avidity of anti-Tau nAbs and relative levels of nAbs towards the major aggregation protein, Tau, in PSP patients in comparison to HCs.

We hypothesize that an impaired humoral immunity (possibly B-cell defects) resulting in Ab affinity/avidity deficiencies can lead to impaired clearance of Tau aggregates, and elimination of damaged brain cells leading to neuroinflammation and neurodegeneration in PSP patients. The hypothesis is formulated based on the laboratory's earlier findings showing significantly decreased levels of high affinity/avidity anti-α-syn nAbs in plasma from PD patients in comparison to HCs, which could potentially play a role in the progression of the pathology in PD. In the same study, Brudek et al. 2017 found a nearly absence of high affinity/avidity anti-α-syn nAbs in plasma from MSA patients in comparison to HCs, which could correspond to a more rapid disease progression seen in MSA (Brudek et al., 2017). In another study, aberrant levels of IgG1-4 subclasses and IgM were found in PD and MSA patients in comparison to HCs. This could support the evidence in impaired immune responses, and the pattern of the specific classes of α-syn nAbs suggests distinctive disease processes in the peripheral immune pathogenesis in these disorders (Folke et al., 2019).

5.1 A decrease in apparent affinity/avidity of nAbs towards Tau and P-Tau in PSP patients

We investigated the apparent affinity/avidity of anti-Tau nAbs and anti-P-Tau nAbs in plasma samples from PSP patients vs. HCs. Identifying the binding plasma fraction of high and low affinity/avidity anti-Tau and anti-P-Tau nAbs were done using a two-site model fitting (Fit logIC50). In this case the model assumes that there are two fractions of nAbs with different affinities/avidities towards a given antigen. In the initial experiments using pooled plasma samples from PSP patients and HCs, we observed a distinctive difference in the affinity/avidity of anti-Tau nAbs profiles, indicated in the inhibition curve patterns (Figure 12A and C). An overall increased percentage of maximum binding was observed in plasma samples from PSP patients, indicating a decrease in the high affinity/avidity anti-Tau nAbs. However, in the initial experiments with P-Tau a comparable inhibition patterns were observed in the pooled plasma samples from PSP patients and HCs, indicating similar affinity/avidity profiles of anti-P-Tau

nAbs (Figure 13). Further, using the optimized competition assay on individual plasma samples, we showed that HCs are characterised by approximately equal levels of low and high affinity/avidity binding components, while in PSP patients, we observed a significantly decreased fraction of high affinity/avidity anti-Tau nAbs. To our surprise we also observed a decrease in the high affinity/avidity fraction of anti-P-Tau nAbs in PSP patients in comparison with HCs.

Previous studies performed in our laboratory, have shown a similar decrease in the apparent of high affinity/avidity nAbs towards α-syn in patients suffering from PD and MSA (Brudek et al., 2017) or towards TDP-43 in patients suffering from ALS (Kallehauge et al., in review). Moreover, in recent Master thesis projects from the laboratory have shown decrease in levels of high affinity/avidity anti-α-syn nAbs in prodromal samples from PD and MSA patients and anti-TDP-43 nAbs in prodromal samples from ALS patients. These observations may indicate a decline in the immune responses towards pathological proteins occurring already prior the disease onset (Emil Bergholt, MCs, unpublished; Sanne Lindberg, MCs, unpublished). These findings may suggest that a decline in the immune response towards amyloidogenic proteins could be a common phenomenon in neurodegenerative disorders, which apparently also applies to PSP.

The immune clearance is a functional system combined of several mechanisms. Due to the natively unfolded structure, Tau is prone for degradation by proteasome, although posttranslational modification and proteolytic cleavage of Tau into smaller fragments can push the degradation of Tau towards the autophagy system (Chesser et al., 2013). Evidence suggest that these two systems are impaired in AD, which could lead to accumulation of Tau fragments, that are prone for aggregation. Moreover, specific posttranslational modified Tau that is not cleared may further contribute to inhibition of the clearance system (Chesser et al., 2013). *In vitro* experiment has been used to determine the uptake of Tau by microglia cells that are the primary phagocytotic cells in the brain. Anti-Tau nAbs are able to mediate intracellular degradation of Tau, however, dysfunctional lysosome acidification can hinder the clearance of Tau (Andersson et al., 2019; Chesser et al., 2013). The decrease in apparent high affinity/avidity of anti-Tau nAbs in PSP could essentially reduce the uptake of Tau by microglia cells resulting in accumulation and enhanced seeding of Tau. Even though an uptake is partially mediated by low affinity anti-Tau nAbs together with the impaired lysosomal function, both could contribute

to intracellular accumulation of Tau. Anti-Tau nAbs are targeting specific altered, misfolded, and aggregated Tau that under normally conditions are cleared within the CNS (Gold et al., 2012). A disruption in the blood-brain barrier (BBB) in PSP could increase levels of aggregated Tau in the circulatory system, and a peripheral immune response may generate Tau reactive Abs that can diffuse over the BBB which may contribute to disease progression and inflammatory responses (Hromadkova & Ovsepian, 2019). A study showing elevated activation of microglia were found in affected brain regions in PSP, and the elevated activation of microglia cells were to some extent correlated with high burden of Tau, which may be supporting evidence for an impaired clearance system (Ishizawa & Dickson, 2001).

Several studies have investigated the levels of nAbs towards different pathological proteins. The levels of anti-α-syn nAbs in serum from PD patients were decreased in comparison with HCs and AD patients, and no difference was found between HCs and AD patients (Besong-Agbo et al., 2013). A decrease of the levels of anti-Aβ nAbs were found in AD patients compared to HCs (Weksler et al., 2002). However, it is not only important to characterize the blood titers of nAbs towards pathological proteins, but the affinity and avidity of nAbs are utmost importance in the clearance of pathological proteins. Multiple studies have investigated the affinity/avidity of pathological proteins similar to PSP in neurodegenerative disorders. It was found that the avidity of anti-Aβ nAbs were decreased in AD patients in comparison with HCs (Jianping et al., 2006), as mentioned earlier in the discussion, a decrease in apparent high affinity/avidity anti-TDP-43 nAbs in ALS in comparison with HCs (Kallehauge et al., in review), and a decrease in apparent high affinity/avidity of anti-α-syn in PD and MSA compared with HCs (Brudek et al., 2017). These studies support the evidence that a decrease in nAbs and their affinity/avidity may have a protective effect towards accumulating and aggregating proteins. In generally, high affinity Abs form more stable bonds to the antigen and provide better protective efficacy (Devey et al., 1984), thus a decrease in high affinity/avidity nAbs may have immunopathological implications.

It has been implied that the accumulation of Tau in the brain may have an important role in the increasing permeability of the BBB found in some neurodegenerative disorders, like AD and PSP (Blair et al., 2015). This dysfunction of the BBB might lead to increased plasma levels of Tau and P-Tau in the blood, nevertheless, it might also be a major part in the disease progression. Increased permeability of the BBB enables immune cells, proteins and other

components to migrate over the endothelium into the brain, leading most probably to increased neuroinflammation. Neurons and glia cells have been shown to produce an increased amount of interleukin-2 (IL-2) in PSP patients and an increased mRNA expression of *GSK3β* was detected in PSP brain samples. Both, IL-2 and GSK3β are regulators of immune cells (Beurel et al., 2010; Rydbirk et al., 2019). These two proteins have been associated with other neurodegenerative disorders like AD and PD (Dansokho et al., 2016; Golpich et al., 2015). Brain imaging has shown an increased microglia activity in PSP patients compared to HCs, which further indicates an increase in inflammatory responses in the brain (Gerhard et al., 2006).

5.2 Cross binding reaction and specifies of anti-Tau nAbs

It has been suggested that nAbs are polyreactive and therefore anti-Tau nAbs may not be epitope specific for Tau. Albus and colleagues published in 2018 that nAbs towards amyloid-beta (Aβ), α-syn and, prion protein found in Creutzfeldt-Jakob disease, possibly recognize the same structural epitopes but with a different affinity, however, only nAbs towards α-syn recognized the structural epitope of α-syn protein (Albus et al., 2018). Therefore, we investigated the cross reaction of anti-Tau nAbs by competition with TDP-43 and α-syn monomers. We found no inhibition of anti-Tau nAbs when competing with TDP-43 and α-syn, which indicates nAbs towards Tau are specific towards structural epitopes on Tau protein (Figure 16). However, we cannot fully exclude at this point that anti-Tau nAbs are able to recognize other proteins with similar structural epitopes to Tau.

Neurodegenerative diseases are frequently presenting an aggregation of more than one pathological protein. AD is primarily represented with extracellular amyloid-beta plaques but Tau aggregates are co-existing in the neuropathology (Spires-Jones et al., 2017). PD pathology is characterized by intracellular aggregated and phosphorylated α-syn forming Lewy bodies, known as synucleinopathy. However, P-Tau aggregates are often co-existing in PD and some studies suggest Tau is co-localized with α-syn in the same cellular inclusions (Moussaud et al., 2014). Interestingly, skin of PD and PSP patients reflects the brain pathology showing disease specific patterns of P-Tau and α-syn accumulation (Rodríguez-Leyva et al., 2016). Therefore, we investigated the apparent high affinity/avidity nAbs towards α-syn in pooled plasma samples from PSP, MSA, ALS patients and HCs. We found an overall increase in the percentage of maximum binding obtained by anti-α-syn nAbs in MSA and PSP patients compared with ALS patients and HCs (Figure 17). This overall increase of maximum binding was expected for MSA

because it is a synucleinopathy and previous studies have shown a decrease in the high affinity/avidity of nAbs towards α-syn in MSA patients compared with HCs (Brudek et al., 2017). α-syn aggregation is associated with ageing and increased levels of α-syn in PSP may be age-dependent (Hsiao-Yuan Lee et al., 2018), nevertheless, this experiment was performed on pooled plasma samples and further validation is needed using individual plasma samples. If our preliminary observation of an impaired immune responses towards α-syn in PSP is valid, it could explain higher levels of a-syn circulating the PSP blood compared to HCs (Hsiao-Yuan Lee et al., 2018). It is worth mention that a co-expression of Tau and α-syn have been suggested to have a strong synergistic effect on neurodegeneration and the interacting of Tau and α-syn may promote pathogenesis through different mechanisms (Moussaud et al., 2014). Tau protein co-aggregates with α-syn in catecholaminergic neurons of PSP brains suggesting a synergistic interaction between the two proteins (Mori et al., 2002). However, the presence of Lewy bodies in PSP is not a common feature (Aguirre et al., 2015). Thus, we can only speculate that increase in Tau and α-syn in some PSP patients and impaired autoantibody responses towards these proteins, may contribute to the disease progression and propagation.

5.3 Increased levels of relative anti-Tau IgG1 in PSP patients without any differences in the global levels of IgG1-4 subclasses, total IgG, and IgM

Investigating the relative levels of anti-Tau IgG1-4 subclasses, total IgG, and IgM using indirect ELISA, we only found increased levels of anti-Tau IgG1 in plasma samples from PSP patients compared with HCs. This observation may be another evidence for increased immunoreactivity towards Tau in PSP patients. However, it remains elusive why the clearance of the protein is dysfunctional. Different Abs promote different immune functions and IgGs can penetrate the tissue and activate the complement system. They can also bind Fc receptors on resident immune cells like macrophages and $CD65^{+}$ natural killer cells (Rydbirk et al., 2019). IgG1 is a potent activator of the complement system mediated by C1 (Veerhuis et al., 2011; Vidarsson et al., 2014). The increased IgG1 found in PSP patients could potentially be part in the increase of microglia activation (Gerhard et al., 2006) due to the binding properties of IgG1 Fc region with Fcγ receptors on the cell surface as well as activation of the complement system. Fcγ receptors are found on both microglia cells and macrophages. Greater activation of microglia cells might induce more secretory pro-inflammatory cytokines/chemokines, resulting in tissue damage in the CNS (Fuller et al., 2014). *In vitro* study provided evidence that Ab interacting with low affinity Fcγ receptor is needed for antibody-mediated clearance of Tau (Andersson et al., 2019).

Thus, the increased levels IgG1 found in PSP patients indicate immune responses but downstream of the response a process in clearance of Tau aggregates is affected, which may support the evidence of an impaired clearance system.

Another reason for a reduction of high affinity/avidity anti-Tau and anti-P-Tau nAbs, could potential be an effect of elevated levels of total Tau and P-Tau circulating in the blood and thereby, resulting in greater pressure on the clearance system and increased antigen-antibody interactions which are not accounted for when measuring free nAbs. Consequently, decreasing the apparent of high affinity/avidity anti-Tau and anti-P-Tau nAbs in PSP patients. The increased levels of relative IgG1 in PSP could be an explanation for the higher levels of immunocomplexes. Tau levels in blood are found to be increased in PSP patients compared to HCs (Hsiao-Yuan Lee et al., 2018), although the results obtained need further validation. Several research groups are currently exploring a new and more sensitive technology for measuring blood titers of Tau. It is a general problem to detect blood content of Tau because of the very low concentrations which are out of the detection range for commercial immunoassays (Hsiao-Yuan Lee et al., 2018; Kronimus et al., 2016; Lue et al., 2019). Hence, it cannot be ruled out that accumulation of P-Tau is caused by an impaired immune response towards Tau and P-Tau and that nAbs have an utmost important protective effect in the pathogenesis.

The clearance mediated by the low avidity nAbs is not as efficient as the one mediated by the high avidity nAbs. High avidity nAbs are forming more stable immunocomplexes (Devey et al., 1984). Moreover, impaired clearance could lead to an over exposure of antigen to the immune system, which may generate a tolerance that could result in an inefficient T cell response (Jianping et al., 2006), resulting in an inadequate B cell immune tolerance that may be the reason for low avidity nAbs and elevated levels of Tau in the circulating blood (Jianping et al., 2006; Weksler et al., 2002). However, a recent study found an increase in $CD4^+$ T cells in PSP blood (Rydbirk et al., 2019). $CD4^+$ T cells play a crucial role in stimulating effective B cell responses and production of Abs (Crotty, 2015) that could explain the increased levels of anti-IgG1 found in PSP. Overall, these and the present results suggest an involvement of the peripheral immune system in PSP.

5.4 Anti-Tau nAbs as a potential biomarker and treatment strategy for PSP

Several studies have been performed to improve and find new treatment strategies in tauopathies, through modifying gene expression of Tau, targeting mechanisms involved in propagation, as well as passive and active Tau vaccines (Jadhav et al., 2019; Uemura et al., 2020). Several ongoing trials are exploring active and passive Tau vaccines, both as preclinical studies and phase 2 studies (ALZFORUM, 2020; Sigurdsson, 2018). Both methods have brought concerns in whether passive vaccines are targeting the right epitopes, due to elusive evidence to which form of Tau that are toxic. On the other hand, active vaccines may provoke excessive uncontrolled immune responses (Sigurdsson, 2018). *In vivo* study observed Ab recognition of a specific epitope on Tau with promising binding properties for AD hyperphosphorylated Tau, as well as potently prevention of Tau seeding (Rosenqvist et al., 2018). However, more studies are needed to investigate anti-Tau nAbs as a treatment strategy with an epitope specific anti-Tau towards aggregated Tau and oligomers to limit clearance of all Tau and maintain normal physiological conditions (Rosenqvist et al., 2018). It is also important to consider the responses mediated by nAbs, i.e. activation of Fcγ receptors that may induce pro-inflammatory cytokines and chemokines which might damage the tissue (Fuller et al., 2014).

It is difficult to diagnose PSP in early stages and the diagnostic value of some biomarkers are questioned and it have been difficult to give the correct diagnosis without sufficiently confirm the diagnose by autopsy (Boxer et al., 2017). Magnetic resonance imaging is widely used as a imaging biomarker for diagnosing PSP, measuring specific brain area ratio but it has proven difficult to distinguish from other neurogenerative disorder like corticobasal degeneration or distinguish PSP phenotypes (Alster et al., 2020; Boxer et al., 2017). Positron emission tomography (PET) is used to investigate specific Tau ligands as a biomarker for diagnosis of neurodegenerative disorders, however, tracers have shown off-target binding in the areas affected in PSP patients. Therefore, more validation and optimization need to be done before PET is suitable for clinical incorporation (Leuzy et al., 2019). Cerebrospinal fluid and blood biomarkers have been investigated, in which neurofilament light chain (NfL) have proven most reliable (Boxer et al., 2017). NfL is a product of damaged myelinated axons and have been explored as a potential biomarker for a diagnostic tool and to predict disease progression in PSP (Rojas et al., 2018). It has been correlated to disease severity but not in the disease progression, however, higher blood levels of NfL are also found in other neurodegenerative

disease, like MSA (Hansson et al., 2017; Rojas et al., 2018). Therefore, a decrease in high affinity/avidity nAbs towards Tau and P-Tau could be a potential biomarker as a diagnostic tool in combination with the level of NfL levels in the blood.

In this study we did not find any correlation between the proportion of affinity/avidity anti-Tau nAbs and disease duration or disease severity. This might suggest the disease progression for PSP is not determined by nAbs, however, anti-Tau and anti-P-Tau nAbs might still contribute to disease progression. Even though no correlation was found between anti-Tau and anti-P-Tau nAbs titers and disease duration or disease severity, it is important to consider the variables that might change the physical and immunological conditions, like age-dependent changes and the indirect effects mediated by medication.

6. Conclusion

In the present study we found a decrease of high affinity/avidity anti-Tau and P-Tau nAbs in plasma samples from PSP patients in comparison with HCs. This finding suggests an impaired clearance system of the pathological protein, Tau. Thus, Tau aggregations in the PSP patients may be a consequence of reduced levels of high affinity/avidity anti-Tau nAbs, which normally clear misfolded and aggregated proteins to maintain homeostasis. High affinity/avidity anti-Tau nAbs might be a potent immunotherapeutic agent in the treatment strategies for PSP patients, however, more human clinical studies is needed. Furthermore, we found increased levels of anti-Tau IgG1 in plasma samples from PSP patients compared with HCs. This suggests that the immune system is responding to altered Tau but insufficiently leading to neuroinflammation and in result to neurodegeneration.

7. Future work

It would be interesting to investigate the levels of immunocomplexes of anti-Tau nAbs/Tau/P-Tau in plasma samples, using sandwich ELISA, as well as measure total Tau and P-Tau levels. In this way it would be possible to quantify whether the decrease in high affinity/avidity nAbs are due to the more immunocomplexes. Another interesting further work is to investigate the avidity of nAbs towards Tau by using indirect ELISA and treat the plasma samples with urea, which disrupts the antigen-antibody interaction. It would be interesting to provide a better stereological display of the neuronal cell loss in the different regions that are affected in PSP, as well as further investigate the expression of cytokines and chemokines in the different regions of the brain as well as in the periphery. Finally, a thorough characterization of lymphocyte populations using flowcytometry, measuring the different types of cells by tagging with a fluorescent membrane marker i.e. CD8, CD4, CD20 and CD16 etc. For the future studies it would be meaningful to isolate B1-cell populations producing anti-Tau nAbs from PSP patients and healthy controls. These approaches would allow to characterize and, in the end, to generate Abs that improve clearance of aggregated Tau.

8. Reference

Aguirre, M. E. E., Zelaya, M. V., de Gordoa, J. S. R., Tuñón, M. T., & Lanciego, J. L. (2015). Midbrain catecholaminergic neurons co-express α-synuclein and tau in progressive supranuclear palsy. *Frontiers in Neuroanatomy*, *9*. https://doi.org/10.3389/fnana.2015.00025

Albus, A., Gold, M., Bach, J. P., Burg-Roderfeld, M., Jördens, M., Kirchhein, Y., … Dodel, R. (2018). Extending the functional characteristics of naturally occurring autoantibodies against β-Amyloid, Prion Protein and α-Synuclein. *PLoS ONE*, *13*(8). https://doi.org/10.1371/journal.pone.0202954

Alster, P., Madetko, N., Koziorowski, D., & Friedman, A. (2020). Progressive Supranuclear Palsy—Parkinsonism Predominant (PSP-P)—A Clinical Challenge at the Boundaries of PSP and Parkinson's Disease (PD). *Frontiers in Neurology*, *11*(180), 1–8. https://doi.org/10.3389/fneur.2020.00180

ALZFORUM. (2020, April 15). Active Tau Vaccine: Hints of Slowing Neurodegeneration. Retrieved July 30, 2020, from https://www.alzforum.org/news/conference-coverage/active-tau-vaccine-hints-slowing-neurodegeneration

Andersson, C. R., Falsig, J., Stavenhagen, J. B., Christensen, S., Kartberg, F., Rosenqvist, N., … Torleif Pedersen, J. (2019). Antibody-mediated clearance of tau in primary mouse microglial cultures requires Fcγ-receptor binding and functional lysosomes. *Scientific Reports*, *9*(1). https://doi.org/10.1038/s41598-019-41105-4

Armstrong, M. J. (2018). Progressive Supranuclear Palsy: an Update. *Current Neurology and Neuroscience Reports*, *18*(3), 1–9. https://doi.org/10.1007/s11910-018-0819-5

Barbier, P., Zejneli, O., Martinho, M., Lasorsa, A., Belle, V., Smet-Nocca, C., … Landrieu, I. (2019). Role of tau as a microtubule-associated protein: Structural and functional aspects. *Frontiers in Aging Neuroscience*, *11*(204), 1–14. https://doi.org/10.3389/fnagi.2019.00204

Basinger, H., & Hogg, J. P. (2019). *Neuroanatomy, Brainstem*. *StatPearls*. Retrieved from http://www.ncbi.nlm.nih.gov/pubmed/31335017

Besong-Agbo, D., Wolf, E., Jessen, F., Oechsner, M., Hametner, E., Poewe, W., … Dodel, R. (2013). Naturally occurring α-synuclein autoantibody levels are lower in patients with Parkinson disease. *Neurology*, *80*(2), 169–175. https://doi.org/10.1212/WNL.0b013e31827b90d1

Beurel, E., Michalek, S. M., & Jope, R. S. (2010). Innate and adaptive immune responses regulated by glycogen synthase kinase-3 (GSK3). *Trends Immunol*, *31*(1), 24. https://doi.org/10.1016/j.it.2009.09.007

Blair, L. J., Frauen, H. D., Zhang, B., Nordhues, B. A., Bijan, S., Lin, Y.-C., … Dickey, C. A. (2015). Tau depletion prevents progressive blood-brain barrier damage in a mouse model of tauopathy. *Acta Neuropathologica Communications*, *3*(8). https://doi.org/10.1186/s40478-015-0186-2

Boxer, A. L., Lang, A. E., Grossman, M., David, S., Miller, B. L., Schneider, L. S., … Gozes, I. (2014). Davunetide for Progressive Supranuclear Palsy: a multicenter, randomized, double-blind, placebo controlled trial. *Lancet Neurology*, *13*(7), 676–685. https://doi.org/10.1016/S1474-4422(14)70088-2.

Boxer, A. L., Yu, J.-T., Golbe, L. I., Litvan, I., Lang, A. E., & Höglinger, G. U. (2017). New diagnostics and therapeutics for progressive supranuclear palsy. *Lancet Neurol*, *16*(7), 552–563. https://doi.org/10.1016/S1474-4422(17)30157-6

Brudek, T., Winge, K., Folke, J., Christensen, S., Fog, K., Pakkenberg, B., & Pedersen, L. Ø. (2017). Autoimmune antibody decline in Parkinson's disease and Multiple System Atrophy; a step towards immunotherapeutic strategies. *Molecular Neurodegeneration*, *12*(1), 1–16. https://doi.org/10.1186/s13024-017-0187-7

Chaplin, D. D. (2010). Overview of the Immune Response. *The Journal of Allergy and Clinical Immunology*, *125*(2), 3–23. https://doi.org/10.1016/j.jaci.2009.12.980

Chen, Y., Park, Y.-B., Patel, E., & Silverman, G. J. (2009). IgM Antibodies to Apoptosis-Associated Determinants Recruit C1q and Enhance Dendritic Cell Phagocytosis of Apoptotic Cells. *The Journal of Immunology*, *128*(10), 6031–6043. https://doi.org/10.4049/jimmunol.0804191

Chesser, A. S., Pritchard, S. M., & Johnson, G. V. W. (2013). Tau clearance mechanisms and their possible role in the pathogenesis of Alzheimer disease. *Frontiers in Neurology*, *4*(122). https://doi.org/10.3389/fneur.2013.00122

Chiu, M. L., Goulet, D. R., Teplyakov, A., & Gilliland, G. L. (2019). Antibody Structure and Function: The Basis for Engineering Therapeutics. *Antibodies*, *8*(4). https://doi.org/10.3390/antib8040055

Crotty, S. (2015). A brief history of T cell help to B cells . *Nat Rev Immunol*, *15*(3), 185–189. https://doi.org/10.1038/nri3803

Dansokho, C., Ahmed, D. A., Aid, S., Toly-Ndour, C., Chaigneau, T., Calle, V., … Dorothé, G. (2016). Regulatory T cells delay disease progression in Alzheimer-like pathology. *Brain*, *139*, 1237–1251. https://doi.org/10.1093/brain/awv408

Desai, A., & Michison, T. J. (1997). Microtubule polymerization dynamics. *Annual Review of Cell and Developmental Biology*, *13*, 83–117.

Devey, M. E., Bleasdale, K., Stanley, C., & Steward, M. W. (1984). Failure of affinity maturation leads to increased susceptibility to immune complex glomerulonephritis. *Immunology*, *52*, 383.

Dickson, D. W., Rademakers, R., & Hutton, M. L. (2007). Progressive supranuclear palsy: Pathology and genetics. *Brain Pathology*, *17*, 74–82. https://doi.org/10.1111/j.1750-3639.2007.00054

Eibel, H., Kraus, H., Sic, H., Kienzler, A.-K., & Rizzi, M. (2014). B cell Biology: An Overview. *Current Allergy and Asthma Reports*, *14*(5), 1–10. https://doi.org/10.1007/s11882-014-0434-8

Enzyme Substrates for ELISA | Thermo Fisher Scientific - DK. (n.d.). Retrieved July 24, 2020, from https://www.thermofisher.com/dk/en/home/life-science/protein-biology/protein-assays-analysis/elisa/elisa-reagents-buffers/enzyme-substrates-elisa.html

Folke, J., Rydbirk, R., Løkkegaard, A., Salvesen, L., Hejl, A.-M., Starhof, C., … Brudek, T. (2019). Distinct Autoimmune Anti-α-Synuclein Antibody Patterns in Multiple System Atrophy and Parkinson's Disease. *Frontiers in Immunology*, *10*(2253). https://doi.org/10.3389/fimmu.2019.02253

Fuller, J. P., Stavenhagen, J. B., & Teeling, J. L. (2014). New roles for Fc receptors in neurodegeneration-the impact on Immunotherapy for Alzheimer's Disease. *Frontiers in Neuroscience*, *8*(235). https://doi.org/10.3389/fnins.2014.00235

Gao, Y., Wang, N., Sun, F., Cao, X., Zhang, W., & Yu, J. (2018). Tau in neurodegenerative disease. *Annals of Translational Medicine*, *6*(10), 1–13. https://doi.org/10.21037/atm.2018.04.23

Gerhard, A., Trender-Gerhard, I., Turkheimer, F., Quinn, N. P., Bhatia, K. P., & Brooks, D. J. (2006). In vivo imaging of microglial activation with [11C](R)-PK11195 PET in progressive supranuclear palsy. *Movement Disorders*, *21*(1), 89–93. https://doi.org/10.1002/mds.20668

Gold, M., Pul, R., Bach, J. P., Stangel, M., & Dodel, R. (2012). Pathogenic and physiological autoantibodies in the central nervous system. *Immunological Reviews*, *248*(1), 68–86. https://doi.org/10.1111/j.1600-065X.2012.01128.x

Golpich, M., Amini, E., Hemmati, F., Ibrahim, N. M., Rahmani, B., Mohamed, Z., … Ahmadiani, A. (2015). Glycogen synthase kinase-3 beta (GSK-3B) signaling: Implications for Parkinson's disease. *Pharmalogical Research*, *97*, 16–26. https://doi.org/10.1016/j.phrs.2015.03.010

Gong, C. X., & Iqbal, K. (2008). Hyperphosphorylation of Microtubule-Associated Protein Tau: A Promising Therapeutic Target for Alzheimer Disease. *Current Medicinal Chemistry*, *15*(23), 2321–2328. https://doi.org/10.2174/092986708785909111

Guo, T., Noble, W., & Hanger, D. P. (2017). Roles of tau protein in health and disease. *Acta Neuropathologica*, *133*(5), 665–704. https://doi.org/10.1007/s00401-017-1707-9

Hanger, D. P., Anderton, B. H., & Noble, W. (2009, March). Tau phosphorylation: the therapeutic challenge for neurodegenerative disease. *Trends in Molecular Medicine*. https://doi.org/10.1016/j.molmed.2009.01.003

Hanger, D. P., Byers, H. L., Wray, S., Leung, K.-Y., Saxton, M. J., Seereeram, A., … Anderton, B. H. (2007). Novel Phosphorylation Sites in Tau from Alzheimer Brain Support a Role for Casein Kinase 1 in Disease Pathogenesis. *The Journal of Biological Chemistry*, *282*(32), 23645–23654. https://doi.org/10.1074/jbc.M703269200

Hansson, O., Janelidze, S., Hall, S., Magdalinou, N., Lees, A. J., Andreasson, U., … Blennow, K. (2017). Blood-based NfL A biomarker for differential diagnosis of parkinsonian disorder. *Neurology*, *88*(10), 930–937. https://doi.org/10.1212/WNL.0000000000003680

Hato, T., & Dagher, P. C. (2015). How the innate immune system senses trouble and causes trouble. *Clinical Journal of the American Society of Nephrology*, *10*(8), 1459–1469. https://doi.org/10.2215/CJN.04680514

Heinisch, J. J., & Brandt, R. (2016). Signaling pathways and posttranslational modifications of tau in Alzheimer's disease: The humanization of yeast cells. *Microbial Cell*, *3*(4), 135–146. https://doi.org/10.15698/mic2016.04.489

Höglinger, Günter U., Huppertz, H. J., Wagenpfeil, S., Andrés, M. V., Belloch, V., León, T., & del Ser, T. (2014). Tideglusib reduces progression of brain atrophy in progressive supranuclear palsy in a randomized trial. *Movement Disorders*, *29*(4), 479–487. https://doi.org/10.1002/mds.25815

Höglinger, Günter U., Melhem, N. M., Dickson, D. W., Sleiman, P. M. A., Wang, L. S., Klei, L., … Zecchinelli, A. L. (2011). Identification of common variants influencing risk of the tauopathy progressive supranuclear palsy. *Nature Genetics*, *43*(7), 699–705. https://doi.org/10.1038/ng.859

Höglinger, Gunter U, Respondek, G., Stamelou, M., Kurz, C., Josephs, K. A., Lang, A. E., … Pellegrin, H. (2017). Clinical Diagnosis of Progressive Supranuclear Palsy: The Movement Disorder Society Criteria. *Mov Disord*, *32*(6), 853–864. https://doi.org/10.1002/mds.26987

Holodick, N. E., Rodríguez-Zhurbenko, N., & Hernández, A. M. (2017). Defining natural antibodies. *Frontiers*

in Immunology, *8*(872). https://doi.org/10.3389/fimmu.2017.00872

Hromadkova, L., & Ovsepian, S. V. (2019). Tau-Reactive Endogenous Antibodies: Origin, Functionality, and Implications for the Pathophysiology of Alzheimer's Disease. *Journal of Immunology Research*, *2019*. https://doi.org/10.1155/2019/7406810

Hsiao-Yuan Lee, E., Wang, Y., Chiu, M.-J., Lin, C.-H., Yang, S.-Y., Horng, H.-E., … Liu, B.-H. (2018). Plasma Biomarkers Differentiate Parkinson's Disease From Atypical Parkinsonism Syndromes. *Frontiers in Aging Neuroscience*, *10*(123). https://doi.org/10.3389/fnagi.2018.00123

Im, S. Y., Kim, Y. E., & Kim, Y. J. (2015). Genetics of progressive supranuclear palsy. *Journal of Movement Disorder*, *8*(3), 122–129. https://doi.org/10.1016/S0072-9752(07)01244-4

Ishizawa, K., & Dickson, D. W. (2001). Microglial Activation Parallels System Degeneration in Progressive Supranuclear Palsy and Corticobasal Degeneration. *Journal of Neuropathology and Experimental Neurology*, *60*(6), 647–657.

Jadhav, S., Avila, J., Schöll, M., Kovacs, G. G., Kövari, E., Skrabana, R., … Zilka, N. (2019). A walk through tau therapeutic strategies. *Acta Neuropathologica Communications*, *7*(1). https://doi.org/10.1186/s40478-019-0664-z

Jeon, G. S., Shim, Y. M., Lee, D. Y., Kim, J. S., Kang, M. J., Ahn, S. H., … Sung, J. J. (2019). Pathological Modification of TDP-43 in Amyotrophic Lateral Sclerosis with SOD1 Mutations. *Molecular Neurobiology*, *56*(3), 2007–2021. https://doi.org/10.1007/s12035-018-1218-2

Jianping, L., Zhibing, Y., Wei, Q., Zhikai, C., Jie, X., & Jinbiao, L. (2006). Low avidity and level of serum anti-Aβ antibodies in Alzheimer disease. *Alzheimer Disease and Associated Disorders*, *20*(3), 127–132. https://doi.org/10.1097/00002093-200607000-00001

Kawai, T., & Akira, S. (2011). Toll-like Receptors and Their Crosstalk with Other Innate Receptors in Infection and Immunity. *Immunity*, *34*(5), 637–650. https://doi.org/10.1016/j.immuni.2011.05.006

Kondělková, K., Vokurková, D., Krejsek, J., Borská, L., Fiala, Z., & Ctirad, A. (2010). Regulatory T cells (TREG) and their roles in immune system with respect to immunopathological disorders. *Acta Medica*, *53*(2), 73–77. https://doi.org/10.14712/18059694.2016.63

Kronimus, Y, Dodel, R., & Neumann, S. (2018). A quantitative view on naturally occurring autoantibodies in neurodegenerative diseases. *Journal of Neurology and Neuromedicine*, *3*(4), 5–11. Retrieved from https://www.jneurology.com/articles/a-quantitative-view-on-naturally-occurring-autoantibodies-in-neurodegenerative-diseases.pdf

Kronimus, Yannick, Albus, A., Balzer-Geldsetzer, M., Straub, S., Semler, E., Otto, M., … Mengel, D. (2016). Naturally Occurring Autoantibodies against Tau Protein Are Reduced in Parkinson's Disease Dementia. *PLOS ONE* , *11*(11), 1–15. https://doi.org/10.1371/journal.pone.0164953

Lacovich, V., Espindola, S. L., Alloatti, M., Pozo Devoto, V., Cromberg, L. E., C ˇ arná, M. E., … Falzone, T. L. (2017). Tau Isoforms Imbalance Impairs the Axonal Transport of the Amyloid Precursor Protein in Human Neurons. *The Journal of Neuroscience*, *37*(1), 58–69. https://doi.org/10.1523/JNEUROSCI.2305-16.2016

Lanciego, J. L., Luquin, N., & Obeso, J. A. (2012). Functional neuroanatomy of the basal ganglia. *Cold Spring Harbor Perspectives in Medicine*, *2*(12). https://doi.org/10.1101/cshperspect.a009621

Leuzy, A., Chiotis, K., Lemoine, L., Gillberg, P.-G., Almkvist, O., Rodriguez-Vieitez, E., & Nordberg, A. (2019). Tau PET imaging in neurodegenerative tauopathies - still a challenge. *Molecular Psychiatry*, *24*, 1112–1134. https://doi.org/10.1038/s41380-018-0342-8

Levin, J., Kurz, A., Arzberger, T., Giese, A., & Höglinger, G. U. (2016). The Differential Diagnosis and Treatment of Atypical Parkinsonism. *Deutsches Arzteblatt International*, *113*(5), 61–69. https://doi.org/10.3238/arztebl.2016.0061

Liu, F., Li, B., Tung, E.-J., Grundke-Iqbal, I., Iqbal, K., & Gong, C.-X. (2007). Site-specific effects of tau phosphorylation on its microtubule assembly activity and self-aggregation. *European Journal of Neuroscience*, *26*(12), 3429–3436. https://doi.org/10.1111/j.1460-9568.2007.05955.x

Lue, L. F., Kuo, Y. M., & Sabbagh, M. (2019). Advance in Plasma AD Core Biomarker Development: Current Findings from Immunomagnetic Reduction-Based SQUID Technology. *Neurology and Therapy*, *8*(2), 95–111. https://doi.org/10.1007/s40120-019-00167-2

MacLeod, M. K. L., Kappler, J. W., & Marrack, P. (2010). Memory CD4 T cells: Generation, reactivation and re-assignment. *Immunology*, *130*(1), 10–15. https://doi.org/10.1111/j.1365-2567.2010.03260.x

Menon, M., Blair, P. A., Isenberg, D. A., & Mauri, C. (2016). A Regulatory Feedback between Plasmacytoid Dendritic Cells and Regulatory B Cells Is Aberrant in Systemic Lupus Erythematosus. *Immunity*, *44*(3), 683–697. https://doi.org/10.1016/j.immuni.2016.02.012

Mori, H., Oda, M., Komori, T., Arai, N., Takanashi, M., Mizutani, T., … Mizuno, Y. (2002). Lewy bodies in progressive supranuclear palsy. *Acta Neuropathologica*, *104*(3), 273–278. https://doi.org/10.1007/s00401-002-0555-3

Moussaud, S., Jones, D. R., Moussaud-Lamodière, E. L., Delenclos, M., Ross, O. A., & Mclean, P. J. (2014). Alpha-synuclein and tau: teammates in neurodegeneration? *Molecular Neurodegenertation*, *9*(43). https://doi.org/10.1186/1750-1326-9-43

MSD. (2014). *FOR RESEARCH USE ONLY. NOT FOR USE IN DIAGNOSTIC OR THERAPEUTIC PROCEDURES*. Retrieved from www.mesoscale.com

MSD. (2019). MSD read buffer t (4x) | Meso Scale Discovery. Retrieved October 21, 2019, from https://www.mesoscale.com/products/msd-read-buffer-t-4x-r92tc/

Murphy, K., & Weaver, C. (2016). *Janeway's Immunobiology* (9th ed.). Garland Science, Taylor & Francis Group. https://doi.org/10.1201/b13424-12

Nath, U., Ben-Shlomo, Y., Thomson, R. G., Morris, H. R., Wood, N. W., Lees, A. J., & Burn, D. J. (2001). The prevalence of progressive supranuclear palsy (Steele-Richardson-Olszewski syndrome) in the UK. *Brain*, *124*(7), 1438–1449. https://doi.org/10.1093/brain/124.7.1438

Natoli, G., & Ostuni, R. (2019). Adaptation and memory in immune responses. *Nature Immunology*, *20*(7). https://doi.org/10.1038/s41590-019-0399-9

Noble, W., Hanger, D. P., Miller, C. C. J., & Lovestone, S. (2013). The importance of tau phosphorylation for neurodegenerative diseases. *Frontiers in Neurology*, *4*. https://doi.org/10.3389/fneur.2013.00083

Orphanet: Progressive supranuclear palsy. (2010). Retrieved September 30, 2019, from https://www.orpha.net/consor/cgi-bin/OC_Exp.php?Expert=683&lng=EN

Owolabi, L. (2013). Progressive supranuclear palsy misdiagnosed as Parkinson's disease: a case report and review of literature. *Annals of Medical and Health Sciences Research*, *3*(Suppl 1), S44-7. https://doi.org/10.4103/2141-9248.121221

Palma, J., Tokarz-Deptuła, B., Deptuła, J., & Deptuła, W. (2018). Natural antibodies – Facts known and unknown. *Central European Journal of Immunology*, *43*(4), 466–475. https://doi.org/10.5114/ceji.2018.81354

Park, H.-J., Lee, K.-W., Oh, S., Yan, R., Zhang, J., Beach, T. G., … Mouradian, M. M. (2018). Protein phosphatase 2A and its methylation modulating enzymes LCMT-1 and PME-1 are dysregulated in tauopathies of progressive supranuclear palsy and Alzheimer disease. *Journal of Neuropathology and Experimental Neurology*, *77*(2), 139–148. https://doi.org/10.1093/jnen/nlx110

Pellegrini, L., Wetzel, A., Grannó, S., Heaton, G., & Harvey, K. (2017, February 1). Back to the tubule: microtubule dynamics in Parkinson's disease. *Cellular and Molecular Life Sciences*. Birkhauser Verlag AG. https://doi.org/10.1007/s00018-016-2351-6

Petersone, L., Edner, N. M., Ovcinnikovs, V., Heuts, F., Ross, E. M., Ntavli, E., … Walker, L. S. K. (2018). T Cell/B Cell Collaboration and Autoimmunity: An Intimate Relationship. *Frontiers in Immunology*, *9*(1941). https://doi.org/10.3389/fimmu.2018.01941

Respondek, G., Stamelou, M., Kurz, C., Ferguson, L. W., Rajput, A., Chiu, W. Z., … Höglinger, G. U. (2014). The phenotypic spectrum of progressive supranuclear palsy: A retrospective multicenter study of 100 definite cases. *Movement Disorders*, *29*(14), 1758–1766. https://doi.org/10.1002/mds.26054

Rodríguez-Leyva, I., Chi-Ahumada, E. G., Carrizales, J., Rodríguez-Violante, M., Velázquez-Osuna, S., Medina-Mier, V., … Jiménez-Capdeville, M. E. (2016). Parkinson disease and progressive supranuclear palsy: protein expression in skin. *Annals of Clinical and Translational Neurology*, *3*(3), 191–199. https://doi.org/10.1002/acn3.285

Rojas, J. C., Bang, J., Lobach, I. V, Tsai, R. M., Rabinovici, G. D., Miller, B. L., & Boxer, A. L. (2018). CSF neurofilament light chain and phosphorylated tau 181 predict disease progression in PSP. *Investigators Neurology*, *90*(4), 273–281. https://doi.org/10.1212/WNL.0000000000004859

Rosenqvist, N., Asuni, A. A., Andersson, C. R., Christensen, S., Daechsel, J. A., Egebjerg, J., … Pedersen, J. T. (2018). Highly specific and selective anti-pS396-tau antibody C10.2 targets seeding-competent tau. *Alzheimer's & Dementia: Translational Research & Clinical Interventions*, *4*, 521–534. https://doi.org/10.1016/j.trci.2018.09.005

Rothstein, T. L., Griffin, D. O., Holodick, N. E., Quach, T. D., & Kaku, H. (2013). Human B-1 cells take the stage. *Annals of the New York Academy of Sciences*, *1285*(1), 97–114. https://doi.org/10.1111/nyas.12137

Rydbirk, R., Elfving, B., Folke, J., Pakkenberg, B., Winge, K., Brudek, T., & Aznar, S. (2019). Increased prefrontal cortex interleukin-2 protein levels and shift in the peripheral t cell population in progressive supranuclear palsy patients. *Scientific Reports*, *9*(1). https://doi.org/10.1038/s41598-019-44234-y

Saiz, M. L., Rocha-Perugini, V., & Sánchez-Madrid, F. (2018). Tetraspanins as organizers of antigen-presenting cell function. *Frontiers in Immunology*, *9*(1074). https://doi.org/10.3389/fimmu.2018.01074

Sathe, A., & Cusick, J. K. (2020). Immunoglobulin M (IgM). In *Biochemistry StatPearls* (pp. 1–16). StatPearls Publishing, Tresure Island (FL). Retrieved from

https://www.ncbi.nlm.nih.gov/books/NBK555995/#!po=84.3750

Scientific, T. F. (n.d.). Overview of ELISA. Retrieved February 24, 2020, from https://www.thermofisher.com/dk/en/home/life-science/protein-biology/protein-biology-learning-center/protein-biology-resource-library/pierce-protein-methods/overview-elisa.html#2

Seifert, M., & Küppers, R. (2016). Human memory B cells. *Leukemia*, *30*, 2283–2292. https://doi.org/10.1038/leu.2016.226

Shahani, N., & Brandt, R. (2002). Functions and malfunctions of the tau proteins. *Cellular and Molecular Life Sciences*, *59*, 1668–1680.

Shi, Z., Zhang, Q., Yan, H., Yang, Y., Wang, P., Zhang, Y., … Qiu, X. (2019). More than one antibody of individual B cells revealed by single-cell immune profiling. *Cell Discovery*, *5*(64), 1–13. https://doi.org/10.1038/s41421-019-0137-3

Shoeibi, A., Olfati, N., & Litvan, I. (2019). Frontrunner in translation: Progressive supranuclear palsy. *Frontiers in Neurology*, *10*. https://doi.org/10.3389/fneur.2019.01125

Sigurdsson, E. M. (2018). Tau Immunotherapies for Alzheimer's Disease and Related Tauopathies: Progress and Potential Pitfalls. *J Alzheimers Dis.* , *64*, 555–565. https://doi.org/10.3233/JAD-179937

Spires-Jones, T. L., Attems, J., & Thal, D. R. (2017). Interactions of pathological proteins in neurodegenerative diseases. *Acta Neuropathologica*, *134*(2), 187–205. https://doi.org/10.1007/s00401-017-1709-7

Stamelou, M., De Silva, R., Arias-Carrión, O., Boura, E., Höllerhage, M., Oertel, W. H., … Höglinger, G. U. (2010). Rational therapeutic approaches to progressive supranuclear palsy. *Brain A Journal of Neurology*, *133*(6), 1578–1590. https://doi.org/10.1093/brain/awq115

Stebegg, M., Kumar, S. D., Silva-Cayetano, A., Fonseca, V. R., Linterman, M. A., & Graca, L. (2018). Regulation of the germinal center response. *Frontiers in Immunology*, *9*(2469). https://doi.org/10.3389/fimmu.2018.02469

Tolosa, E., Litvan, I., Höglinger, G. U., Burn, D., Lees, A., Andrés, M. V., … del Ser, T. (2014). A phase 2 trial of the GSK-3 inhibitor tideglusib in progressive supranuclear palsy. *Movement Disorders*, *29*(4), 470–478. https://doi.org/10.1002/mds.25824

Trushina, N. I., Bakota, L., Mulkidjanian, A. Y., & Brandt, R. (2019). The Evolution of Tau Phosphorylation and Interactions. *Frontiers in Aging Neuroscience*, *11*. https://doi.org/10.3389/fnagi.2019.00256

Uemura, N., Uemura, M. T., Luk, K. C., Lee, V. M. Y., & Trojanowski, J. Q. (2020). Cell-to-Cell Transmission of Tau and α-Synuclein. *Trends in Molecular Medicine*, 1–17. https://doi.org/10.1016/j.molmed.2020.03.012

Vacchio, M. S., & Bosselut, R. (2016). What Happens in the Thymus Does Not Stay in the Thymus: How T Cells Recycle the CD4 + –CD8 + Lineage Commitment Transcriptional Circuitry To Control Their Function . *The Journal of Immunology*, *196*(12), 4848–4856. https://doi.org/10.4049/jimmunol.1600415

Veerhuis, R., Nielsen, H. M., & Tenner, A. J. (2011). Complement in the Brain. *Mol Immunol*, *48*(14), 1592–1603. https://doi.org/10.1016/j.molimm.2011.04.003

Venkatramani, A., & Panda, D. (2019). Regulation of neuronal microtubule dynamics by tau: Implications for tauopathies. *International Journal of Biological Macromolecules*. https://doi.org/10.1016/j.ijbiomac.2019.04.120

Vidarsson, G., Dekkers, G., & Rispens, T. (2014). IgG subclasses and allotypes: From structure to effector functions. *Frontiers in Immunology*. https://doi.org/10.3389/fimmu.2014.00520

Wang, Y., & Mandelkow, E. (2016). Tau in physiology and pathology. *Nature Reviews Neuroscience*, *17*(1), 5–21. https://doi.org/10.1038/nrn.2015.1

Weksler, M. E., Relkin, N., Turkenich, R., LaRusse, S., Zhou, L., & Szabo, P. (2002). Patients with Alzeimer disease have lower levels of serum anti-amyloid peptide antibodies than health elderly individuals. *Experimental Gerontology*, *37*(7), 943–948. https://doi.org/10.1016/S0531-5565(02)00029-3

Winkelstein, J. A. (1973). Opsonins: Their function, identity, and clinical significance. *The Journal of Pediatrics*, *82*(5), 747–753. https://doi.org/10.1016/S0022-3476(73)80062-9

Wong, J. B., Hewitt, S. L., Heltemes-Harris, L. M., Mandal, M., Johnson, K., Rajewsky, K., … Skok, J. A. (2019). B-1a cells acquire their unique characteristics by bypassing the pre-BCR selection stage. *Nature Communications*, *10*(1). https://doi.org/10.1038/s41467-019-12824-z

Wood, P. (2011). *Understanding Immunology* (Third). Pearson Education Limited.

Workman, C. J., Szymczak-Workman, A. L., Collison, L. W., Pillai, M. R., & Vignali, D. A. A. (2009). The development and function of regulatory T cells. *Cellular and Molecular Life Sciences*, *66*(16), 2603–2622. https://doi.org/10.1007/s00018-009-0026-2

Wray, S., Saxton, M., Anderton, B. H., & Hanger, D. P. (2008). Direct analysis of tau from PSP brain identifies new phosphorylation sites and a major fragment of N-terminally cleaved tau containing four microtubule-binding repeats. *Journal of Neurochemistry*, *105*(6), 2343–2352. https://doi.org/10.1111/j.1471-4159.2008.05321.x

Yamasaki, T. R., Holmes, B. B., Furman, J. L., Dhavale, D. D., Su, B. W., Song, E. S., … Diamond, M. I. (2019). Parkinson's disease and multiple system atrophy have distinct a-synuclein seed characteristics. *Journal of Biological Chemistry*, *294*(3), 1045–1058. https://doi.org/10.1074/jbc.RA118.004471

Zhang, N., & Bevan, M. J. (2011). CD8+ T Cells: Foot Soldiers of the Immune System. *Immunity*, *35*(2), 161–168. https://doi.org/10.1016/j.immuni.2011.07.010

Appendix 1

Demographic characteristics of Progressive Supranuclear Palsy patients.

Gender	H&Y	Age	Age of onset	Disease duration	FU level of diagnosis
Male	-	61	55	6	Probable
Female	3	66	61	5	Probable
Male	3	63	58	5	Probable
Female	-	58	55	3	Probable
Female	-	61	56	5	Probable
Male	-	70	59	11	Probable
Male	-	62	51	11	Probable
Male	-	70	65	5	Possible
Male	-	64	58	6	Probable
Male	-	65	51	14	Probable
Female	-	61	56	5	Probable
Male	-	74	69	5	Probable
Male	4	74	73	1	Probable
Male	3	63	60	3	Probable
Female	3	63	60	3	Probable
Male	2	64	58	6	Probable
Male	3	69	68	1	Probable
Female	4	69	59	10	Probable
Male	4.5	75	96	6	Probable
Male	4	79	76	3	Probable
Female	3	65	64	1	Probable
Female	3	67	54	13	Probable
Female	3	66	61	5	Probable
Male	3	71	65	6	Probable
Female	-	72	67	5	Possible
Male	4	61	54	7	Probable
Male	3	73	68	5	Probable

Female	-	65	60	5	Probable
Male	3	74	67	7	Probable
Female	3	65	63	2	Probable
Male	-	58	47	11	Possible
Male	4	71	68	3	Probable
Male	-	81	70	11	Possible
Male	-	70	59	11	Possible
Female	3	74	71	3	Possible
Male	3	66	65	1	Probable
Male	3	75	74	1	Probable
Male	3	69	60	9	Probable
Female	3	78	74	4	Probable
Male	4	69	64	5	Probable
Male	5	58	47	11	Probable
Male	3	62	58	4	Probable
Male	4	78	74	4	Probable
Male	5	74	66	8	Probable
Female	3	73	70	3	Probable
Male	3	62	58	4	Probable
Male	5	70	63	7	Probable
Male	3	76	71	5	Possible
Male	4	71	68	3	Probable
Female	3	71	68	3	Possible
Male	3	68	67	1	Possible
Male	4	69	64	5	Possible
Female	3	65	63	2	Possible
Female	4	7	70	2	Probable
Male	4	72	71	1	Probable

Appendix 2

Correlation between the affinity/avidity of anti-Tau nAbs and Hoehn & Yahr scale or disease duration.

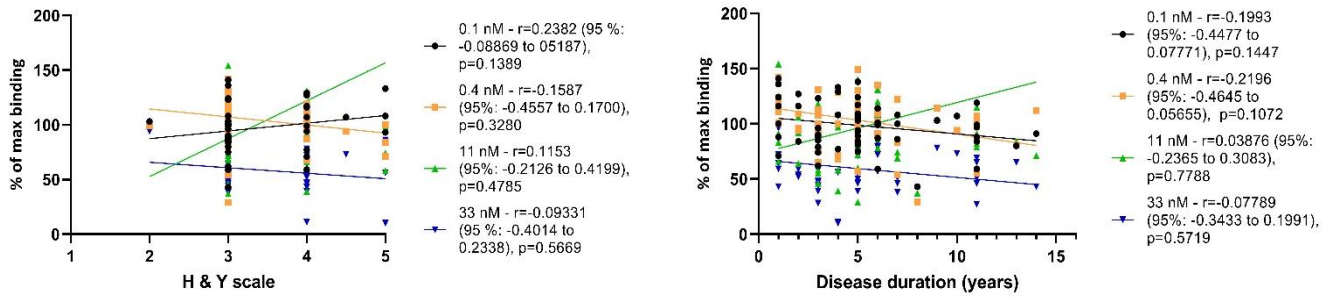

Figure I | ***Correlation between affinity/avidity of anti-Tau nAbs and Hoehn & Yahr scale and disease duration.*** *The y-axis shows the % of maximum binding and x-axis shows Hoehn & Yahr (H & Y) scale (left) or disease duration (years) (right). For each concentration 0.1 nM (black), 0.4 nM (yellow), 11 nM (green), and 33 nM (blue), the r- value, 95 % confidence, and p- value are shown.*

Appendix 3

Correlation between the affinity/avidity of anti-P-Tau nAbs and Hoehn & Yahr scale or disease duration.

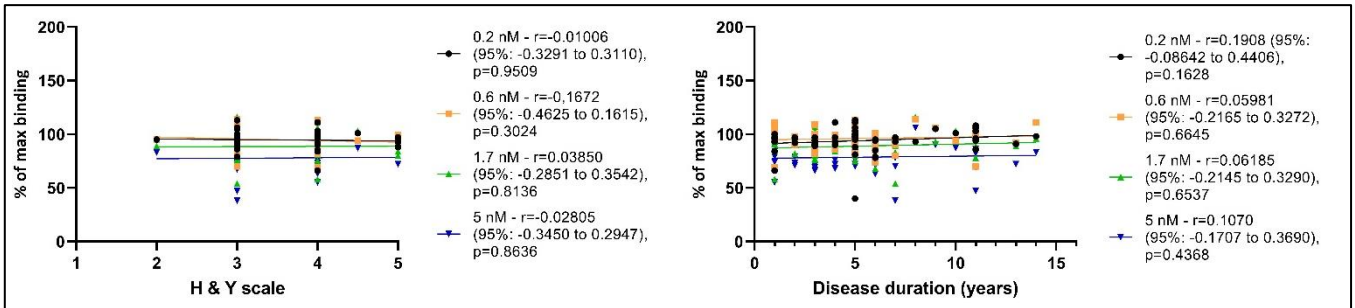

Figure II | ***Correlation between affinity/avidity of anti-P-Tau nAbs and Hoehn & Yahr scale and disease duration.*** *The y-axis shows the % of maximum binding and x-axis shows Hoehn & Yahr (H & Y) scale (left) or disease duration (years) (right). For each concentration 0.2 nM (black), 0.6 nM (yellow), 1.7 nM (green), and 5 nM (blue), the r- value, 95 % confidence, and p- value are shown.*

Appendix 4

ELISA optimization for measurement of relative levels of anti-IgG1-4. Through optimization of ELISA we examined different secondary antibodies, blocking buffers, and dilution buffers. The same procedure was used as described in the report.

The first secondary antibodies tested were:

- Human IgG1 Fc, HRPO conjugated, Cat. No. MH1715 (Invitrogen, USA)
- Mouse anti-human IgG2 Rd, HRP conjugated, Cat. No. MH1722 (Invitrogen, USA)
- Mouse anti-human IgG3 (heavy chain) secondary antibody HRP conjugated, Cat. No. 05-3620 (Invitrogen, USA)
- Mouse anti-human IgG4 Fc secondary antibody, Cat. No. MH1742 (Invitrogen, USA)

The plate was coated with different Tau concentration: 0.1 µg/ml (red), 0.05 µg/ml (blue), or 0.01 µg/ml (green) and incubated overnight. The plates were block with PBS + 3 % BSA + 0.1 % NP-40 and washed three times with PBS + 0.1 % tween. Pooled plasma samples were diluted 1:50 in 0.1% BSA + PBS. Secondary antibodies were diluted 1:100, 1:200, 1:500, and 1:1000 in 0.1 % BSA + PBS (Figure III). See ELISA protocol for more details.

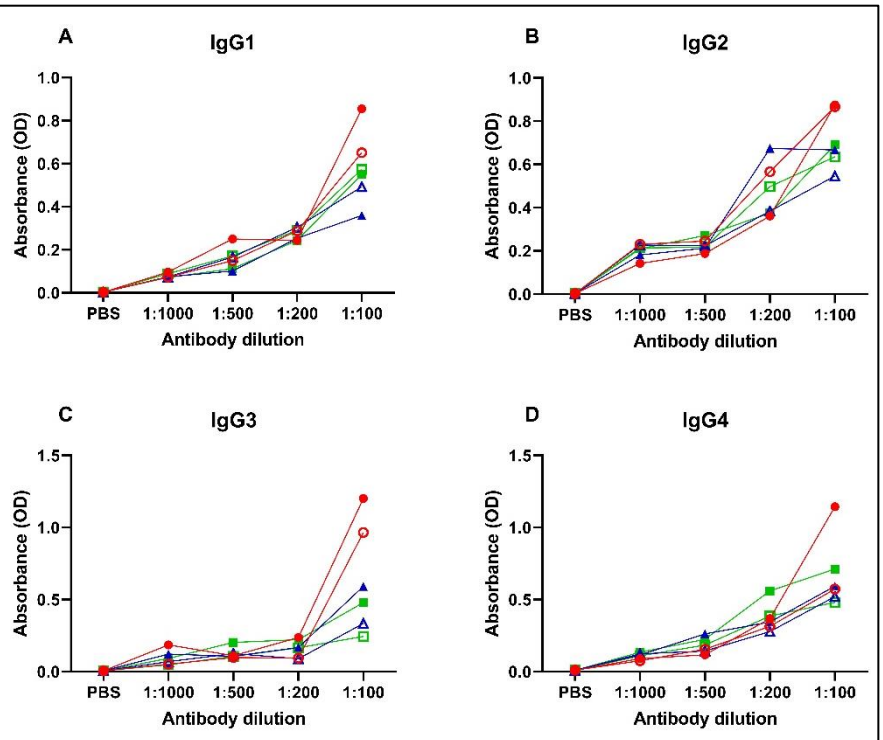

Figure III | ***Graphs of the absorbance (OD) obtained during the optimization using secondary antibodies from Invitrogen.*** *Y-axis represent the absorbance (OD) and x-axis represents the different dilutions of* ***A.*** *anti-IgG1,* ***B.*** *anti-IgG2,* ***C.*** *anti-IgG3, and* ***D.*** *anti-IgG4. The different coating concentrations are 0.1 ng/ml (red), 0.05 ng/ml (blue), and 0.01 ng/ml (green). The wells are treated with either 1:50 plasma (Circles, triangle, and square) or with PBS (white-circle, white-triangle, and white-square).*

The wells are either treated with 1:50 plasma (circle, triangle, and square) or with PBS + 0.1 % BSA (white-circle, white-triangle, and white-square) and then incubated with different dilutions of secondary antibody. As seen in Figure III the measured absorbance when treating the wells with PBS + 0.1 % BSA the OD is almost equal and sometimes higher when comparing the OD when treated with 1:50 pooled plasma. Indicating there was a lot of unspecific binding to the plate. This was a recurrent problem and we decided to try some new secondary HRP conjugated antibodies.

The second secondary antibodies tested were:

- Mouse monoclonal Anti-human IgG1 hinge heavy chain HRP conjugate (500µl), Cat. No. ab99774 (Abcam)
- Mouse monoclonal anti-human IgG2 Fc, HRP conjugated (500µl), Cat. No. ab99779 (Abcam)
- Mouse anti-human IgG3, HRP conjugated, Cat. No. LS-C70322 (Nordic Biosite)
- Mouse anti-human IgG4 pFc', HRP conjugate (500µl), Cat. No. ab99817 (Abcam)

The plate was coated with different Tau concentration: 0.1 µg/ml (red), 0.05 µg/ml (blue), or 0.01 µg/ml (green) and incubated overnight. The plates were block with PBS + 3 % BSA + 0.1

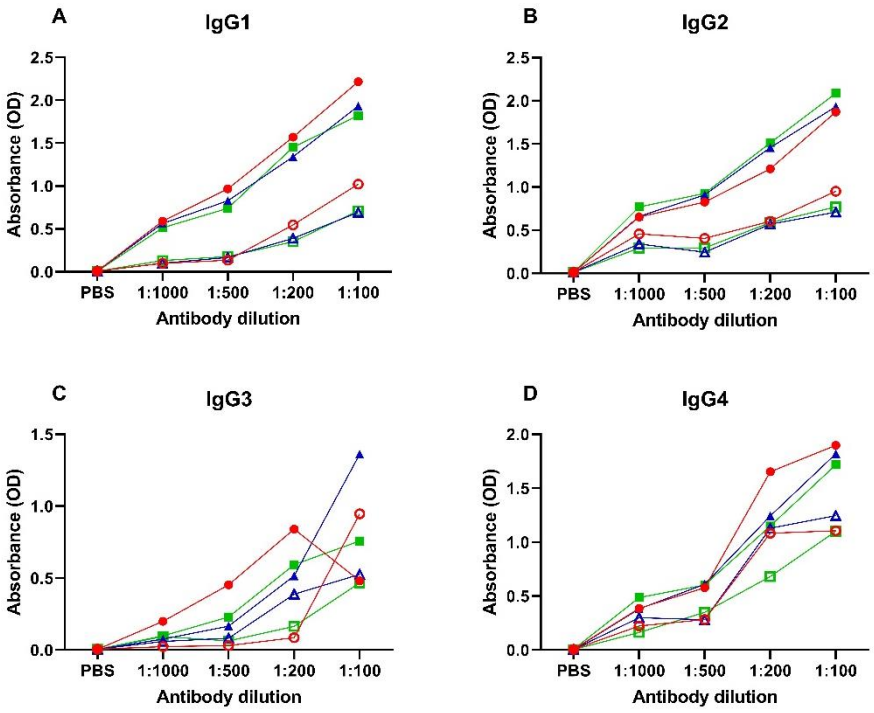

Figure IV | ***Graphs of the absorbance (OD) obtained during the optimization using secondary antibodies from Abcam and Nordic Biosite.*** *Y-axis represent the absorbance (OD) and x-axis represents the different dilutions of* ***A.*** *anti-IgG1,* ***B.*** *anti-IgG2,* ***C.*** *anti-IgG3, and* ***D.*** *anti-IgG4. The different coating concentrations are 0.1 ng/ml (red), 0.05 ng/ml (blue), and 0.01 ng/ml (green). The wells are treated with either 1:50 plasma (Circles, triangle, and square) or with PBS (white-circle, white-triangle, and white-square).*

% NP-40 and washed as three times in PBS + 0.1 % tween. Pooled plasma samples were diluted 1:50 in 0.1% BSA + PBS. Secondary antibodies were diluted 1:100, 1:200, 1:500, and 1:1000 in 0.1 % BSA + PBS. See ELISA protocol for more details.

The wells were treated with 1:50 plasma or with PBS + 0.1 % BSA and then treated with secondary antibody in different dilutions (Figure IV). Again, it is seen in Figure IV the OD when treating the wells with PBS + 0.1 % BSA is almost equal and in some cases higher when comparing the OD when treating the wells with 1:50 pooled plasma. There was not much consistency in the measured OD for all the secondary antibodies. Although, the measured OD in anti-IgG1 and anti-IgG2 showed more consistency in the measurement, however the OD when treating the wells with PBS + 0.1 % BSA was still very high. The goal was to obtain an OD around 1 because when the OD is too high or too low the measurement will likely be more uncertain. The high background signal was a recurrent problem, hence we decided trying to use individual samples from PSP patients and HCs, other blocking buffers and another dilution buffer.

Dilution of secondary antibodies and coating concentrations were chosen from the previous results obtained. Hence, the coating concentration were 0.05 µg/ml Tau, plasma dilution 1:50, and secondary antibody dilutions were 1:500 or 1:1000. Figure VFigure shows raw data (OD) when using individual samples from PSP patients (yellow) and HC (blue), as well as wells treated with PBS (white). Wells treated with PBS instead of plasma, gave OD measurements which were not consistent when using the same secondary antibody, which gave some concerns for the reliability of the data.

IgG1	PSP	PBS	HC	PBS
1:50 plasma	1.206	0.258	0.821	0.182
1:500 Ab	0.27	0.238	0.787	0.216
	0.355	0.34	1.171	0.342
	1.302	0.218	0.959	0.5
	0.727	0.172	0.788	0.27
	1.226	0.32	0.754	0.601
IgG2	PSP	PBS	HC	PBS
1:50 plasma	0.535	0.187	0.646	0.151
1:500 Ab	0.923	0.456	0.677	!4.190
	1.101	0.233	1.035	0.275
	3.934	0.178	0.708	0.426
	1.37	0.274	0.513	0.268
	0.601	0.286	1.165	0.34
IgG3	PSP	PBS	HC	PBS
1:50 plasma	0.556	0.371	0.624	0.117
1:1000 Ab	0.485	0.257	0.357	1.369
	2.045	0.276	0.438	0.437
	1.54	0.165	0.479	0.445
	1.021	0.35	0.48	0.36
	0.461	0.385	0.589	0.335
IgG4	PSP	PBS	HC	PBS
1:50 plasma	0.742	0.328	2.04	0.558
1:500 Ab	0.475	0.24	0.372	0.339
	1.516	0.638	0.843	0.517
	0.513	0.368	0.797	0.433
	0.612	0.643	0.796	0.501
	0.545	0.533	0.705	3.041

*Figure V | **An example of raw data (OD) obtained when using individual samples.** The coating concentration was 0.05 µg/ml. Individual plasma samples were diluted 1:50 for PSP patients (Yellow) and health controls (HC) (Blue) and the white columns are treated with PBS. Anti-IgG1, -IgG2, and -IgG4 were diluted 1:500 and -IgG3 was diluted 1:1000.*

Figuring out how to overcome the unspecific binding, we tested multiple blocking buffers: 1 % skim milk powder (Cat. No. 70166, Fluka) diluted in PBS, (1:5) Odyssey® blocking buffer (Cat. No. 927-40000, Li-cor) diluted in PBS, and SuperBlock™ Blocking buffer (Cat. No. 37515, TermoFisher). Another dilution buffer was tested as well; 1 % BSA diluted in PBS. The coating concentration, plasma dilution, and secondary antibodies were not changed.

The results in Figure VI obtained from the different blocking buffers, still showed a lot unspecific binding due to the high OD measured when treating the wells with PBS + 0.1 % BSA (last three rows) instead of 1:50 plasma (First six rows). The most promising was the 1 % skim milk and Odyssey® blocking buffer, but it seemed that the effect of the blocking buffer was affected by which secondary antibody that was used. Comparing the dilution buffers, it did not seem that the 1 % BSA + PBS improved the OD by decreasing the unspecific binding.

		PSP			HC			PBS		
		Skim milk 1%	Superblock	Licor block 1:5	Skim milk 1%	Superblock	Licor block 1:5	Skummælk 1%	Superblock	Licor block 1:5
IgG1	0.1 % BSA	2.38	1.496	1.785	0.693	1.047	0.766	0.864	0.969	1.215
	1 % BSA	1.555	1.247	1.145	1.089	1.266	1.296	1.042	1.667	1.179
IgG2	0.1 % BSA	2.529	2.809	2.746	3.88	2.25	1.453	1.259	1.885	1.425
	1 % BSA	2.705	2.273	2.345	3.823	1.451	1.465	2.116	1.185	1.441
IgG3	0.1 % BSA	0.632	0.48	1.642	0.423	0.456	1.163	0.438	0.759	0.705
	1 % BSA	0.394	0.338	1.175	0.155	0.248	0.433	0.19	0.223	0.515
IgG4	0.1 % BSA	1.106	0.765	1.358	0.707	1.061	1.169	0.829	0.949	1.062
	1 % BSA	0.482	0.311	0.631	0.446	0.49	0.583	0.692	1.039	0.778

*Figure VI | **Raw data (OD) obtained when using individual plasma samples testing three blocking buffers and dilution buffer**. Each group (PSP diluted 1:50, HCs diluted 1:50, and PBS) were tested against 1 % skim milk (red), Superblock (yellow), and 1:5 Licor block (green) as well as the dilution buffers 0.1 % BSA + PBS (blue rows) and 1 % BSA + PBS (white rows) for each of the secondary antibodies. Anti-IgG1, -IgG2, and -IgG4 were diluted 1:500 and anti-IgG3 was diluted 1:1000.*

From these results we decided to test PBS + 3 % skim milk + 0.1 % NP-40 and 1:2 Odyssey® blocking buffer + 0.1 % NP-40 diluted in PBS. Due to previously high OD we diluted the plasma 1:100 in PBS +0.1 % BSA. The anti-IgG1, -IgG2, and -IgG4 were diluted 1:500 and anti-IgG3 was diluted 1:1000 in PBS +0.1 % BSA. The raw data in Figure VII showed slightly improvement when using 3 % skim milk + 0.1 % NP-40 compared to 1:2 Odyssey® blocking buffer + 0.1 % NP-40. The rows that were treated with PBS + 0.1 % BSA (white) showed a lower OD for all secondary antibodies compared with the rows treated with 1:100 plasma dilution (yellow and

3 % Skim milk + 0.1% NP-40											
IgG1			IgG2			IgG3			IgG4		
PSP	HC	PBS	PSP	HC	PBS	PSP	HC	PBS	PSP	HC	PBS
0.565	0.335	0.288	0.504	0.604	0.417	0.537	0.66	0.59	0.83	0.799	0.74
0.829	0.345	0.288	0.633	0.503	0.362	0.629	0.48	0.563	0.715	0.824	0.545
0.927	0.373	0.304	0.476	0.622	0.346	0.483	0.948	0.545	1.444	0.886	0.659
0.602	1.141	0.516	0.646	2.016	0.518	0.709	0.897	0.534	0.662	1.26	0.75
Licor-Block 1:2 + 0.1% NP-40											
IgG1			IgG2			IgG3			IgG4		
PSP	HC	PBS	PSP	HC	PBS	PSP	HC	PBS	PSP	HC	PBS
0.556	0.528	0.575	0.556	0.65	0.562	0.981	0.981	0.512	0.739	0.888	0.652
1.064	0.357	0.333	0.569	0.493	0.454	0.71	0.477	0.375	0.775	0.661	0.416
0.867	0.467	0.394	0.43	0.684	0.505	0.855	1.349	0.381	0.809	0.649	0.498
0.517	1.431	0.52	0.602	0.978	0.505	1.112	0.939	0.457	0.6	0.82	0.437

*Figure VII | **Raw data (OD) obtained when using individual plasma samples testing two blocking buffers.** Each group, PSP diluted 1:100 (yellow), HCs diluted 1:100 (green), and PBS (white) were tested against 3% skim milk + 0.1 % NP-40 (upper part) and 1:2 Licor block + 0.1 % NP-40 (lower part). Anti-IgG1, -IgG2, and -IgG4 were diluted 1:500 and anti-IgG3 was diluted 1:1000.*

green) when blocking with 3 % skim milk + 0.1 % NP-40. When blocking with 1:2 Odyssey® blocking buffer + 0.1 % NP-40 we still saw lower OD when treating with PBS (white) compared with 1:100 plasma dilution (yellow and green).

Both blocking still gave a lot of unspecific binding, hence we decided to test 3 % skim milk + 0.1 % NP-40 and 5 % skim milk + 0.1 % NP-40 diluted in PBS, to compare the two different concentrations of skim milk powder. Comparing the two blcoking buffers there were no differences between the two concentrations of skim milk, as shown in Figure VIII.

3 % Skim milk + 0.1% NP-40											
IgG1			IgG2			IgG3			IgG4		
PSP	HC	PBS	PSP	HC	PBS	PSP	HC	PBS	PSP	HC	PBS
1.058	0.881	0.906	0.611	0.756	0.385	0.506	0.698	0.481	0.877	1.07	0.542
0.75	1.974	0.667	2.161	0.774	0.36	0.577	0.592	0.344	1.168	0.819	0.694
1.36	0.464	0.682	3.03	0.411	0.594	1.984	0.533	0.385	3.764	1.223	0.729
0.835	1.028	0.702	0.652	1.583	0.534	0.621	1.032	0.568	0.974	1.53	1.7
5 % Skim milk + 0.1% NP-40											
IgG1			IgG2			IgG3			IgG4		
PSP	HC	PBS	PSP	HC	PBS	PSP	HC	PBS	PSP	HC	PBS
0.936	0.488	0.603	0.422	0.425	0.508	0.481	0.606	0.543	0.779	1.11	0.995
0.929	1.418	0.316	2.394	0.663	0.302	0.434	0.425	0.38	1.128	0.737	0.786
0.916	0.422	0.262	2.905	0.594	0.463	0.328	1.395	0.475	3.793	0.853	0.803
0.547	0.835	0.591	0.624	1.616	0.651	0.559	0.699	0.435	0.838	1.268	1.048

*Figure VIII | **Raw data (OD) obtained when using individual plasma samples testing two blocking buffers**. Each group, PSP diluted 1:100 (yellow), HCs diluted 1:100 (green), and PBS (white) were tested against 3% skim milk + 0.1 % NP-40 (upper part) and 5% skim milk + 0.1 % NP-40 (lower part). Anti-IgG1, -IgG2, and -IgG4 were diluted 1:500 and -IgG3 was diluted 1:1000.*

Appendix 5

Correlation between the relative OD of anti-IgG1-4 subclasses, -total IgG, and -IgM and Hoehn & Yahr scale or disease duration.

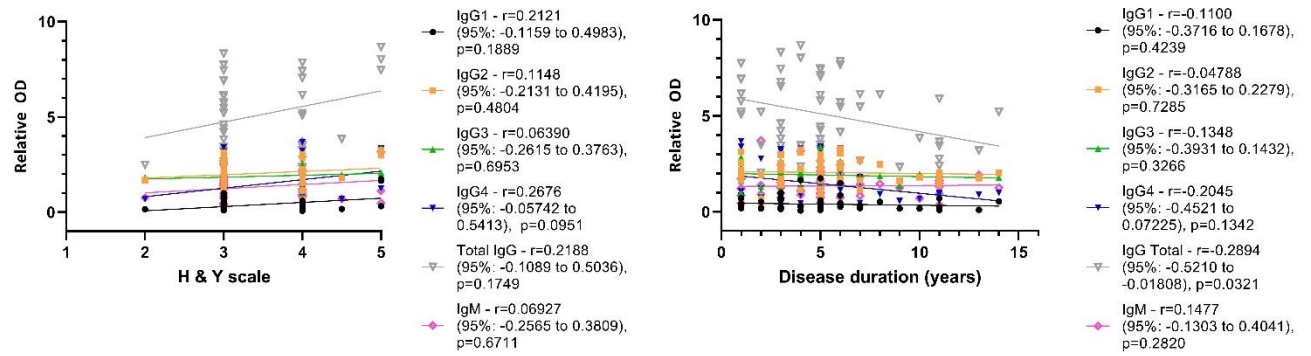

*Figure IX | **Correlation between relative OD and Hoehn & Yahr scale or disease duration.** The y-axis shows relative OD and x-axis shows Hoehn & Yahr (H & Y) scale (left) or disease duration (years) (right). Anti-IgG1 (black), -IgG2 (yellow), -IgG3 (green), -IgG4 (blue), -total IgG (grey), and -IgM (pink), the r- value, 95 % confidence, and p- value are shown.*

Appendix 6

Correlation between the global levels of IgG1-4 subclasses, total IgG, and IgM and Hoehn & Yahr scale or disease duration.

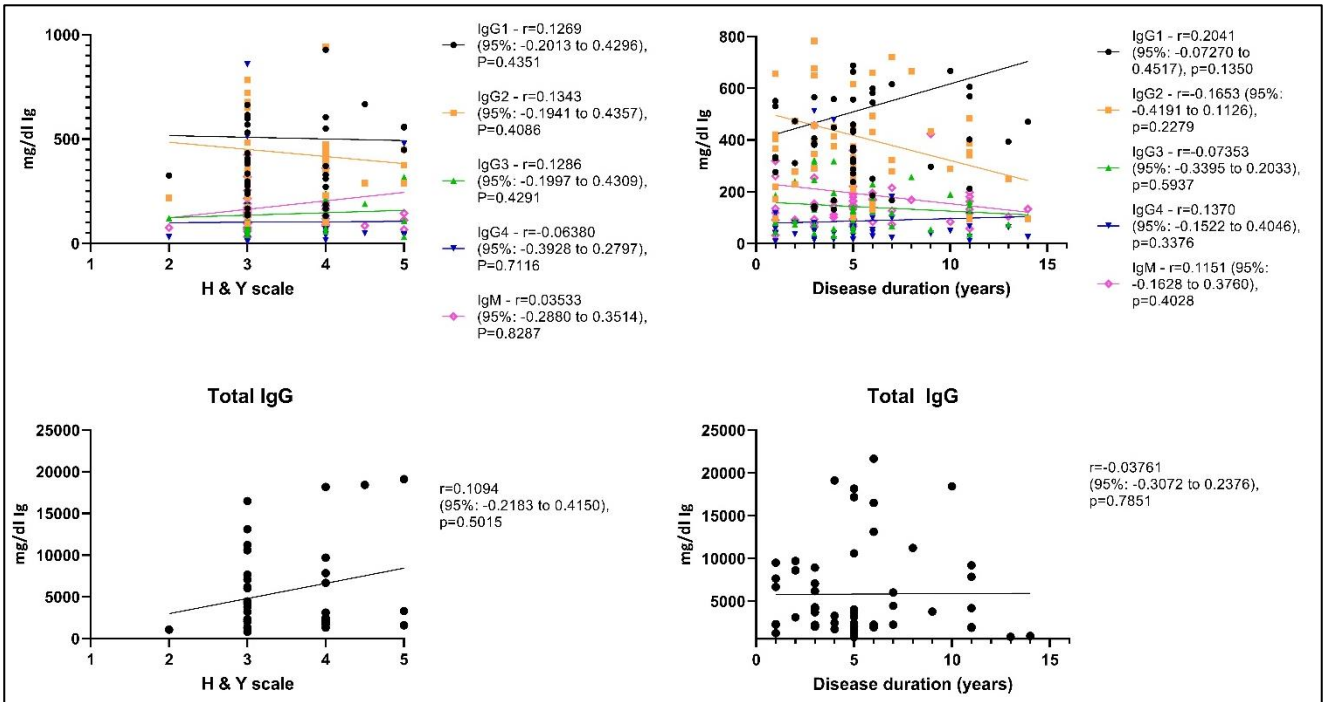

*Figure X | **Correlation between global levels of Igs and Hoehn & Yahr scale or disease duration.** The y-axis shows mg/dl and x-axis shows Hoehn & Yahr (H & Y) scale (left) or disease duration (years) (right). IgG1 (black), IgG2 (yellow), IgG3 (green), IgG4 (blue), and IgM (pink), the r- value, 95 % confidence, and p- value are shown. Total IgG are shown alone in graphs due to the high concentration of Ig.*